Dean, L. E., D. R. Moran, R. D. Hicks, and P. T. Winn, 2024: pressure measurements and video observations near and inside three EF2 tornadoes. *Electronic J. Severe Storms Meteor.*, **19** (2), 1–45.

Electronic Journal of
SEVERE STORMS METEOROLOGY

Pressure Measurements and Video Observations near and inside Three EF2 Tornadoes

LANNY E. DEAN
WeatherBug, PACRITEX, Rogersville, Missouri

DAVID R. MORAN
DTN, PACRITEX, Yukon, Oklahoma

RANDY D. HICKS
PACRITEX, Cave Springs, Missouri

PAT T. WINN
PACRITEX, Mannford, Oklahoma

(Submitted 12 September 2023; in final form 14 August 2024)

ABSTRACT

From the springs of 2016–2019, three EF2-rated tornadoes were sampled with in-situ tornado probes as part of the Pressure Acoustics Recordings Inside Tornadoes Experiment. The probe's meteorological instrumentation resolved the temperature, humidity and pressure-deficit characteristics near or inside the three tornadoes. Probes recorded pressure and visual observations during each tornado event show unique attributes, including multiple strong pressure fluctuations before and just after the first EF2 tornado, and a rotating bowl-shaped cloud feature located some distance ahead of the second EF2 tornado, independent of the tornado core and immediate inflow layer. Pressure measurements of the bowl feature reveal a brief perturbation lasting roughly 4 s as it passed near or directly over the research team before the documentation of a 41-hPa pressure deficit associated with the tornado. During the third EF2 in-situ deployment, pressure-trace observations also reveal fluctuations ahead of the tornado core, lasting some 65 s before the documentation of a 13-hPa pressure deficit associated with the tornado. These measurements and video observations are consistent in location with recent ultra-high-resolution simulations of the streamwise vorticity current (SVC), or more precisely, the related vertical vorticity sheet (VVS) and pressure deficit lobe (PDL) regions. This paper describes the measured pressure-deficit traces during three EF2 tornadoes near and in situ, augmented with brief, one-of-a-kind, near and in-situ video observations of a unique bowl feature, tornado inflow, corner-flow, and tornado core regions. The recorded data and instrumentation were analyzed; results are presented and discussed.

1. Introduction

Longstanding theoretical discussions and previous research have proven the vigorous demands and challenges in obtaining near and in-situ data within tornado cores and supercells (e.g., Bedard and Ramzy 1983; Bluestein 1983; Bluestein et al. 2003; Samaras and Lee 2004; Lee et al. 2004; Lee et al. 2011; Wurman and Samaras 2004; Karstens et al. 2010). Due to these challenges and low success rates, only a limited number of formal in-situ measurements or documentation exists (e.g., Dean et al. 2022, hereafter DMH22; Kosiba and Wurman 2013).

Still, there is a continued need for in-situ observations to help understand tornado-vortex behavior, dynamics and the associated micro-α scale environment. The recent DMH22 documentation of the first-ever in-situ visual observations of the "higher-order multiple

Corresponding author address: Lanny E. Dean, Rogersville, MO. E-mail: led42@msstate.edu

vortices" (Wurman and Kosiba 2013) validate this need. The DMH22 in-situ observations were obtained through years of field research from the privately funded field research campaign called Pressure Acoustics Recordings Inside Tornadoes Experiment (hereafter PACRITEX). Objectives of the PACRITEX field research, as outlined in DMH22, include meteorological, infrasonic, and video documentation near and in situ to tornadoes. This paper is a continuum of the PACRITEX field project, which investigated near and in-situ pressure perturbations thought to be related to the streamwise vorticity current (Orf et al. 2017) during the 2019 severe weather season.

Previous laboratory, numerical and large-eddy simulations (e.g., Ward 1972; Rotunno 1977; 1979; 1984; Lewellen et al. 1997; Lewellen and Lewellen 2007; Schenkman et al. 2014) have helped our understanding of vortex dynamics by offering finescale vortex details, despite inabilities to simulate important atmospheric flow properties (e.g., Ward 1972; Rotunno 1984), domain limitations (e.g., Lewellen et al. 1997), and or spatial resolution limitations (e.g., Schenkman et al. 2014). More recent large-eddy simulation research by Orf et al. (2017, hereafter O17) curbed many of these limitations in providing an ultra-high-resolution (30-m grid spacing) simulation of the 24 May 2011 El Reno, OK supercell, which produced an EF5 tornado.

The O17 findings highlight a feature called the streamwise vorticity current (hereafter SVC), which, in the most basic form, is a horizontally rotating tube flowing helically towards the updraft located on the cool side (along and north) of the front-flank downdraft boundary (hereafter FFDB). O17 suggest this SVC tube is responsible for increasing the streamwise vorticity flowing up and into the low-level mesocyclone (hereafter LLM). As the vorticity increases, the strength of the updraft/LLM increases, thereby increasing rotation within the LLM, as seen in Finely et al. (2018, hereafter F18) and akin to studies by Davies-Jones (1984) and Davies-Jones and Brooks (1993).

As the LLM strengthens, a vertical vorticity sheet (hereafter VVS) is seen in O17 near the FFDB, similar to Markowski et al. (2014), promoting a "train of vortices" flowing towards the updraft-downdraft interface. This parade of vortices, likely caused by vertical shearing near the FFDB, consolidates near the updraft-downdraft interface, facilitating tornadogenesis. At nearly the same time, a pressure-deficit lobe (hereafter PDL) is also seen in the Orf et al. (2018, hereafter O18) simulation, lowering toward the surface (Fig. 1).

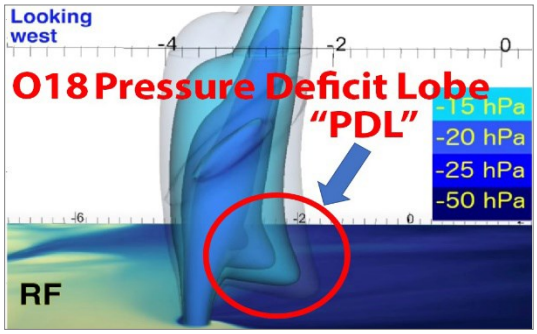

Figure 1: View of the O18 SVC pressure deficit lobe (PDL) post-tornadogenesis, circled in red. View is looking west with the PDL lobing toward the surface. Adapted from Orf et al. (2018) and courtesy of Leigh Orf. *Click to enlarge*.

O18 suggest this PDL is likely caused by a positive feedback loop where the ingestion of vorticity-rich cold-pool air increases the pressure drop, thus causing expeditious strengthening of the LLM at the possible SVC and LLM interface. This process would result in even more vorticity ingestion and parcel stretching (Orf 2023 personal communication). After the O18 embryonic tornado develops, the VVS train of vortices slow their rearward propagation toward the main tornado and LLM, while the PDL continues to lobe out and downward toward the surface during the early maintenance phase, as seen in the O17, O18, and Finley et al. (2023, hereafter F23) simulations.

To the authors' knowledge, the O17 and O18 proposed PDL has not been documented observationally in formal literature. However, Snyder et al. (2013, hereafter S13) documented a small feature using high-resolution mobile X-band radar coined the low-reflectivity ribbon (hereafter LRR), in seven supercells. S13 characterized the LRR as a textured coiling narrow band of reduced reflectivity extending through the front-flank core (likely near the front-flank convergence boundary) to where the front-flank downdraft attaches to the hook echo (Fig. 20 in S13), possibly similar to the DMH22 visual eddy observations (their Fig. 12). S13 radar observations during a supercell on 23 May 2008 in northwest Oklahoma, shows this LRR was comprised of multiple small cyclonic

vortices that quickly moved southward toward and inside of the hook echo (Fig. 11 in S13). While S13 was likely the first to formally highlight the LRR, others have previously documented its presence (e.g., Wurman et al. 2012; Kosiba et al. 2013). Griffin et al. (2018, hereafter G18) further expounded the S13 findings during VORTEX-2 (Wurman et al. 2012), using a suite of in situ sticknets to measure kinematic variables within the LRR. Their observations from three supercells show multiple LRRs with pseudoequivalent temperature and surface pressure changes (i.e., spikes and dips in the surface pressure and temperature (their Figs. 3–6). They also showed the LRR lifecycle through the forming stages, near the FFDB, through decay, near the left-flank convergence boundary and the rear-flank downdraft boundary intersection (their Fig. 21). During the LRR forming stages, G18 found a deformation near/on the FFDB that strongly correlates with the O17 simulation of the VVS. The authors of this study believe this could be related to the origination of the VVS (i.e., inflection point), which seems supported in O17 with this inflection on the FFDB essentially serving as a focus of rearward moving cyclonic vorticity, likely similar to S13 and G18.

Although O17 highlight the SVC, their study was not the first to show the overall importance of streamwise vorticity in updraft rotation. Browning and Landry (1963) theorized that thunderstorm rotation could be the result of tilting of ambient shear vorticity, while early numerical modeling also highlighted the importance of upward titling of horizontal shear vorticity (e.g., Wilhelmson and Klemp 1978; Rotunno 1981: Rotunno and Klemp 1982; Lilly 1982). Klemp and Rotunno (1983) showed areas of strengthening vorticity along/behind the FFDB and identified the flow as mostly parallel to the boundary, leading to horizontal baroclinic vorticity along the path of the inflow parcels. Davies-Jones (1984) corroborated and expanded these findings, showing that streamwise vorticity was indeed the base fundamental driving source of updraft rotation, while Rotunno and Klemp (1985) further showed that horizontal vorticity originating from areas that were baroclinic, as well as the environmental vorticity, were both tilted vertically at the mesocyclone. They also showed that the vertically tilted baroclinically generated horizontal vorticity, ahead or upstream of the LLM, was a main source of low-level rotation in supercells.

More recent studies by Beck and Weiss (2013) identified three main storm-scale boundaries: i) the rear-flank downdraft boundary (RFDB), ii) the left-flank convergence boundary (LFCB), iii) the front-flank convergence boundary (FFCB). They showed streamwise vorticity along both the FFCB and LFCB that was significantly stronger and larger than the environmental vorticity, with parcel trajectories terminating at the LLM, similar to Wicker and Wilhelmson (1995). Dahl et al. (2014) seem to support Beck and Weiss (2013), and found baroclinic generation of crosswise horizontal vorticity, which would then realign with the horizontal velocity vector and become streamwise. Dahl (2017) further simulated two updrafts in an environment with crosswise and mostly streamwise vorticity. Their work showed that the pressure gradient could be changed in a way that horizontal vorticity within the inflow region acquires a large streamwise element even when and if the horizontal vorticity starts off purely crosswise, which seems to be supported in F23. Even so, more recent simulations by Coffer et al. (2023) emphasize the importance of environmental low-level streamwise vorticity versus storm-generated and baroclinically driven. In that study, the low-level inflow parcels bound for LLM originated from the ambient environment, and the absorption of parcels originating within the front-flank were likely a byproduct of dynamic lifting of the strengthening LLM itself.

Despite Coffer et al. (2023) using the level of free convection (LFC) as their baseline, noting issues clarifying the exacts of the lowest near-surface part of the LLM compared to previous studies (e.g., Kelmp and Rotunno 1985), and the likely continued discussion of storm-generated baroclinic vorticity versus environmental, previous field research has likely fortuitously observed or poorly sampled an SVC-like structure (e.g., Markowski et al. 2018). However, Dowell and Bluestein (1997) seem to be the first to have observed a streamwise vorticity feature using research radar during the 17 May 1981 Arcadia, OK F2 tornado, appearing to have similarities to the O17 SVC. Dowell and Bluestein (2002) further found vorticity maxima placement using airborne dual-Doppler radar observations that coincided with horizontal streamwise vorticity on and near an identified FFCB/FFDB, and noted various kinematic boundaries within the forward flank. Markowski et al. (2012) analyzed radar observations, which

showed that the baroclinic streamwise vorticity increased from the northeast of the LLM just after a descending reflectivity core (Rasmussen et al. 2006). This suggests that the LLM inflow was cut off from lesser-quality, negatively buoyant air to the south of the FFCB. Similarly, Kosiba et al. (2013) found horizontal vorticity enhancement along a defined FFCB during the 5 June 2009 Goshen County, WY, tornado. They highlighted that the backward-integrated parcels from the LLM mostly originated along or near the identified FFCB and FFDB, similar to the O17 and O18 simulations. However, until recently, there had been little concrete evidence to suggest that SVCs, as defined in O17, O18, and F18, occur in supercells.

Schueth et al. (2021) compared a simulated supercell to high-resolution mobile radar observations of two supercells, finding evidence that SVCs existed in both observed supercells. Murdzek et al. (2020) used simultaneous dual-Doppler and mobile mesonet observations from three supercells and identified SVCs in two of the three. Additionally, recent findings from Satrio (2023) traced parcel trajectories backward, and found evidence of an SVC during the 17 May 2019 McCook, NE tornado event (an additional focus of this study). The Satrio (2023) vorticity budget supports the O17/O18 notion that the LLM strengthened as a direct response to processes occurring in the forward flank, which would support the role of an SVC-like feature in LLM intensification (e.g., F23). The Satrio (2023) backward-trajectory findings also support the acquisition or generation of baroclinic vorticity as the parcels passed through the forward-flank region [in contrast to the Coffer et al. (2023) simulations], thus showing that not only is the SVC [and possibly the associated VVS feature (e.g., S13; G18; Wurman et al. 2012; Kosiba et al. 2013)] legitimately physical, but also that the storm-generated baroclinic vorticity is critically important to the storm dynamics. Still, it is unknown what percentages of supercells have an SVC, if an SVC is required to be present at all, or what role, if any, the possible SVC might have on the LLM strengthening, tornadogenesis, maintenance, or decay.

While the SVC (as defined by O17) has been identified in recent radar studies (e.g., Murdzek et al. 2020; Schueth et al. 2021; Satrio 2023), and possibly the associated VVS feature (S13; G18), to the best of the authors' knowledge, no formal publications or field research have specifically targeted the O17 and O18 proposed VVS or PDL regions, using ground-based, in-situ tornado probes. Thus, the O18 proposed VVS and PDL became the main objectives of the PACRITEX 2019 field research campaign, which was guided by three questions:

1) Do the O18 vortices within the VVS extend to the ground? The authors realize the S13 and G18 findings of the LLR likely established the VVS vortices as near-surface (i.e., 0–3 km AGL), which is supported by Kosiba et al. (2013) and Wurman et al. (2012); however, we believe the S13 "near-surface" is a bit open-ended.
2) If so, are these VVS vortices visible in situ?
3) Can pressure perturbations or deficits of these VVS vortices or the PDL be measured at the ground in situ?

Owing to the potential relationship between the SVC and the temperature and pressure fields in the forward flank, pressure traces hypothetically might be able to detect these features in the field.

Since the 1950s, many efforts have been made to understand pressure deficits near and in tornadoes, with most early observations usually coming by way of accidental tornado encounters with static barometers (e.g., Lewis and Perkins 1953; Tepper and Eggert 1956). By the mid-1980s, the first deployable ground-based in-situ tornado probe [the Totable Tornado Observatory (TOTO)] had been designed and used in the field in attempts to intentionally sample meteorological variables near and in tornadoes (Bluestein 1983; Bedard and Ramzy 1983). Due to limited success, and because TOTO could be tipped over in windspeed <50 m s^{-1}, efforts to use TOTO were abandoned by the late 1980s (Bluestein 1999). However, the usefulness of deploying a portable instrumented in-situ tornado probe near and in the path of tornadoes was realized, and the development of other smaller/lighter weight in-situ tornado probes ensued, including SNAILS (Tatom et al. 1995), turtles (Brock et al. 1987), E-Turtles (Winn et al. 1999), the Hardened In Situ Tornado Probe (HITPR) designed by the late Tim Samaras (Samaras and Lee 2004), sticknets (Weiss and Schroeder 2008), and pods (Wurman 2008).

Although many of these in-situ probes had varying degrees of success, Winn et al. (1999, hereafter W99) successfully placed two E-Turtle probes on each side of the Allison, Texas F4

tornado on 8 June 1995, and documented pressure-deficits over time. The W99 pressure observations revealed a 50-hPa pressure deficit and the classic V-shape characteristic highlighted in their recorded pressure trace. On 7 May 2002, Tim Samaras deployed an HITPR near the Pratt, KS F2 tornado, also documenting a significant V-shape pressure-deficit signature as a 31-hPa pressure drop was recorded (Samaras and Lee 2004). Additional successful in-situ deployments by Samaras include the Manchester, SD F4 tornado on 24 June 2003, where a 100-hPa pressure deficit was recorded (Lee et al. 2004). The Manchester pressure trace also showed the classic V-shaped signature with interesting pressure fluctuations seen prior to the Manchester tornado impacting the HITPR and the associated 100-hPa pressure deficit. Similar to the Lee et al. (2004) findings, Wurman and Samaras (2004) recorded a large pressure drop and a fascinating pressure trace characterized by multiple smaller V-shaped or U-shaped signatures prior to and during the large V-shaped signature associated with the 15 May 2003 Stratford, TX tornado (discussed further herein).

This paper is not intended to be a historical review discussing all known formal past in-situ observations. Still, detailed comparison and analysis of 21 previous near and in-situ observational cases, in addition to the recorded pressure data described herein, make this case study novel, in that it is believed to be the first study to explicitly investigate and compare those 21 previously recorded in-situ pressure-deficit traces to the recorded data described herein, and the O17, O18, and F23 simulations. The pressure observations described in this study and most, if not all, of the 21 previous in-situ observations were documented in or near regions where O17, O18, and F23 propose the possible SVC VVS and or PDL to be, and also near the LLM. For that reason, this study also discusses the possibility in which the LLM surface pressure falls could be associated with the recorded data herein and the previous 21 in-situ observational cases.

This paper is outlined as follows: section 2 presents the methodology and describes the PACRITEX three near and in-situ deployments. Section 3 describes the in-situ tornado probe, instrumentation, and discusses the probe testing validation. Probe operation is described in section 4. Each tornado case event with video observations (if applicable), recorded pressure traces, analysis, and, in one case, wind velocity, is offered in section 5. Comparison and analysis of previous in-situ pressure-deficit observational studies are discussed in section 6. Section 7 discusses the theoretical concerns and observational considerations of the recorded data herein. This paper concludes with a summary and detailed discussion in section 8.

2. Deployments and methodology

During the 2016–2019 severe weather seasons, the PACRITEX field campaign used in-situ tornado probes (hereafter INPAR probes) to sample tornadoes near and in situ. Thanks to the aerodynamic shape, the INPAR probes have survived several strong to violent tornadoes, including the 16 June 2014 westernmost Pilger, NE EF4 tornado (DMH22). On 30 March 2016, the first author successfully deployed an INPAR probe in the direct path of the Tulsa, OK, EF2-rated tornado, to test fabrication upgrades made to the original DMH22 probe design. Results of the Tulsa recorded pressure trace indicated the INPAR probe could record pressure deficits near and inside tornadoes (Section 5). Additional successful near and in-situ deployments include the 25 May 2016 Chapman, KS EF4 tornado and the 16 May 2017 Elk City, OK EF2 tornado. These data, particularly the Tulsa tornado event, which will be presented in future publications, ultimately led to the PACRITEX 2019 field research campaign and this study.

On 23 February 2019 and 17 May 2019, the PACRITEX research team also intercepted tornadic supercells near Burnsville, MS, and McCook, NE, in attempts to deploy the ground-based INPAR tornado probes in or near the above-described FFCB/FFDB, LFCB, and the O17 proposed VVS and PDL regions. This study highlights the PACRITEX 2019 field research results from the Burnsville, MS EF2 and McCook, NE EF2 tornado events (while also discussing the testing results and data from the Tulsa, OK tornado) and describes the measured in-situ pressure deficit traces, augmented with brief, one-of-a-kind, near and in-situ video observations of a unique rotating bowl-shaped cloud feature, tornado inflow, corner-flow, and tornado core regions.

3. Instrumentation and testing validation

The conically shaped flat-top INPAR probes (Fig. 2a) house meteorological sensors, camera equipment, GPS, and data logging equipment.

Fabrication upgrades from the original DMH22 design were completed in late 2015, and include four shadowboxes that house four GoPro cameras on the lower sides of the probe and a top-mount GoPro camera, for a total of five cameras (Fig. 2b).

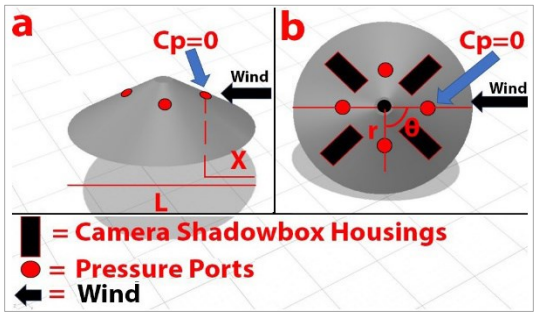

Figure 2: INPAR probe 3D schematic showing a) side view of the X/L, pressure ports, and C_p=0 location, b) INPAR 3D top view showing camera shadowbox housings, pressure ports. The black arrows denote the wind axis.

A single push-button switch activates the INPAR probe with a 5VDC, 19 800-mAh mil-spec rechargeable lithium-ion battery powering all on-board electronics. The INPAR can run up to 16 h before a recharge is needed, and up to 37 h if two batteries are used in tandem. Due to the small file size, sufficient onboard memory allows up to 96 h of data-recording capability (using an external battery) before a data download is required. A Bosch BME280 sensor (Fig. 3a) measures the pressure, temperature, and relative humidity with a normal sampling rate of 1 Hz (up to 40 Hz in forced mode). Forced mode sampling is multiple or single maximum measurements performed in accordance to the selected measurement and sensor filter options, as designated by the user's script and BME280 sensor coding.

The Global Positioning System (GPS) consists of an L80-M39 GPS and Global Orbiting Navigation Satellite System (GLONASS) Stratum 1 receiver (Fig. 3b). The GPS sampling rate was set in normal mode at 1 Hz (up to 40 Hz forced mode). Due to the connection and logging of multiple hardware devices (i.e., BME280 and L80-M39), a Raspberry Pi 3b was used as the data logger (Fig. 3c). The quad-core 1.2-GHz Broadcom CPU can compute many thousands of samples per second, interfaces multiple communication protocols, including SPI, UART and I2C, and has 128 GB of storage. Programming of each device was done with Python (e.g.,https://github.com/boschsensortec/BME280 driver.git; L80-M39 driver /code), and scripts were written for each device. A microbarograph pressure-sensitive switch (Fig. 3d) was employed to detect and measure infrasonic signatures (e.g., Bedard and Georges 2000; Bedard 2005; Georges and Green 1975; Arnold et al. 1976), with the sampling rate set at normal mode of 50 Hz (60 Hz in forced mode). While infrasonic signatures were captured during the Tulsa, OK, Burnsville, MS, and McCook, NE, tornado events, those data will be highlighted in a future publication.

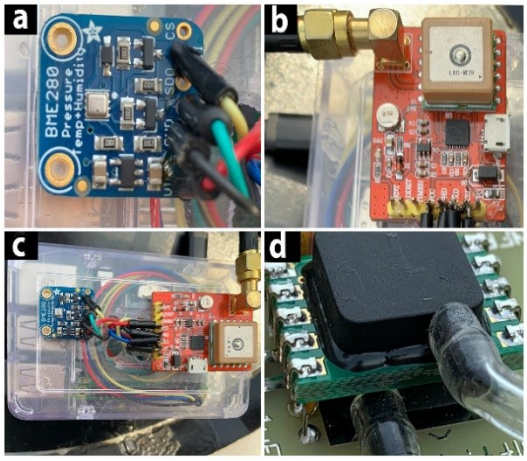

Figure 3: INPAR internal hardware devices: a) BME280 pressure sensor, b) L80-M39 GPS and GLONASS Stratum 1 receiver, c) Raspberry Pi 3b data logger with GPS receiver and BME280 sensor mounted, d) Microbarograph pressure-sensitive switch. *Click to enlarge*.

a. First validity test

Because the Oklahoma mesonet (e.g., Brock et al. 1995) was dubbed "the gold standard" of statewide weather networks by the National Research Council (2009), first validation testing of the INPAR probe commenced on 25 February 2019, two days after the Burnsville, MS tornado deployment, and consisted of a 96-hour pressure comparison test between the Oilton, OK Mesonet site (OILT) and the INPAR. The first author (LD) drove to near the OILT site and emulated an open in-situ deployment (e.g., Lee et al. 2004; Samaras 2006; DMH22; Wurman and Samaras 2004; Winn et al. 1999) by placing the INPAR on the ground, activating it with an attached external battery, and leaving it for 96 h to compare the daily maximum and minimum

pressure values. Although the Oklahoma mesonet suite utilizes Vaisala PTB220 barometers (McPherson et al. 2007) with a notable difference in the pressure sampling rate compared to the INPAR sampling rate [Humidity Sensor BME280 | Bosch Sensortec (bosch-sensortec.com)], the INPAR BME280 and OILT PTB220 share similar but not exact maximum and minimum full scale (hereafter FS) atmospheric pressure-range values (www.mesonet.org/about/instruments), making OILT a good pressure reference testing base. Comparison testing included best-practice FS error metrics used for calculating pressure sensors as noted by Validyne Engineering (Pressure Sensor Accuracy | Validyne Engineering), as can be seen in Eq. (1):

$$\mathrm{PE} = \frac{MP-RP}{FSmax-FSmin} \times 100 \quad (1)$$

Where: PE = percentage error, MP = measured pressure, RP = reference pressure, FS_{max} = full scale maximum, FS_{min} = full scale minimum. Total FS error percentage was then calculated for the entire 96-hour test, as seen in Eq. (2):

$$\mathrm{PE} = \frac{FS_{max}-FS_{min}}{\sum_{i=1}^{4}(MP_i-RP_i)} \times 100 \quad (2)$$

Where: FS_{max} = full scale maximum, FS_{min} = full scale minimum, MP_i = measured pressure for each day (i = days 1–4), RP_i = reference pressure for each day (i = days 1–4).

Comparison between the INPAR and OILT pressure at 5-min intervals throughout the 96-hour pressure test shows the INPAR measured pressure was consistently ≈2–3-hPa higher than the OILT measured pressure (Fig. 4) and that OILT responded more quickly to overall increasing pressure and maximum daily pressure values. However, the INPAR BME280 responded faster to overall decreasing pressure and minimum daily pressure values (Fig. 4).

Error results of the four-day comparison test revealed an average error rate of less than 1.1% difference in the maximum pressure values between the INPAR and the OILT mesonet over the four-day test [as calculated in Eqs. (1) & (2)]. Recorded minimum atmospheric pressure values revealed even less variability with less than 0.3%, or less than 3-hPa difference, in minimum daily pressure values during the four-day comparison test [as calculated in Eqs. (1) and (2)]. Of particular note, the four larger spikes seen in Fig. 4 are believed to be attributed to the first author's manually lifting the probe to approximately waist to chest height, periodically (four times) throughout the 96-hour comparison test to verify the probe connection to the external battery was still on, and that all electronics were still recording. These spikes *might* also be seen in the Tulsa, OK, Burnsville, MS, and McCook, NE, pressure traces, seen as smaller spikes when first deploying the INPAR probes.

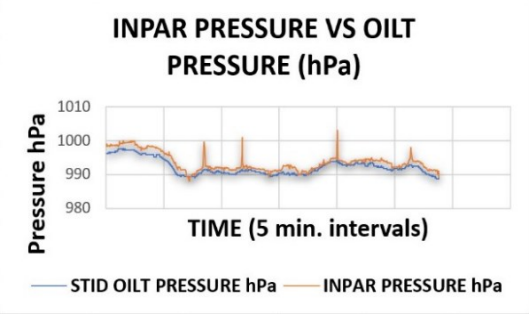

Figure 4: 96-h maximum and minimum daily pressure-test comparison results between the INPAR (orange line) and the Oilton, OK (OILT) Mesonet site (blue line) from 25 February 2019 through 28 February 2019. *Click to enlarge.*

b. Second validity test

INPAR wind-tunnel calibration and validation tests were completed in the spring of 2023 in the Beech wind tunnel in Wichita, KS [Walter H. Beech Wind Tunnel (wichita.edu)]. Pressure variations were measured by applying various wind velocities ranging between 22–55 m s^{-1} across the entire body of the INPAR for 360-degree testing. Upon completing the initial wind-tunnel tests, strong focus was then placed on applying the various wind velocities to the primary wind-facing side of the INPAR probe and pressure ports to validate the quality of the INPAR pressure sensor and to attempt to replicate the Burnsville recorded pressure data results (discussed in Section 5). Figure 5a shows the INPAR wind-tunnel test results through each degree and respective Q (i.e., applied windspeed within the wind tunnel) and the associated wind-tunnel pressure deficits compared to the probe raw results. The error rate of the BME280 pressure sensor was measured across each Q (applied wind-tunnel speed) and then compared with the wind-tunnel pressure variations. The average error rate between the measured wind-tunnel data and the BME280 measured pressure was found at ±3.08-hPa, or near 0.31 % (Fig. 5a).

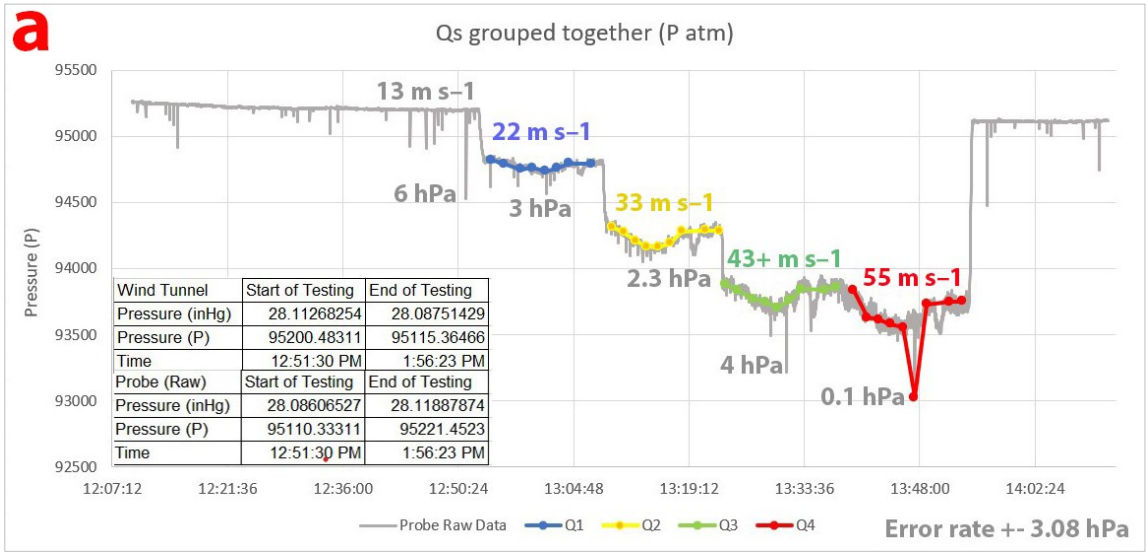

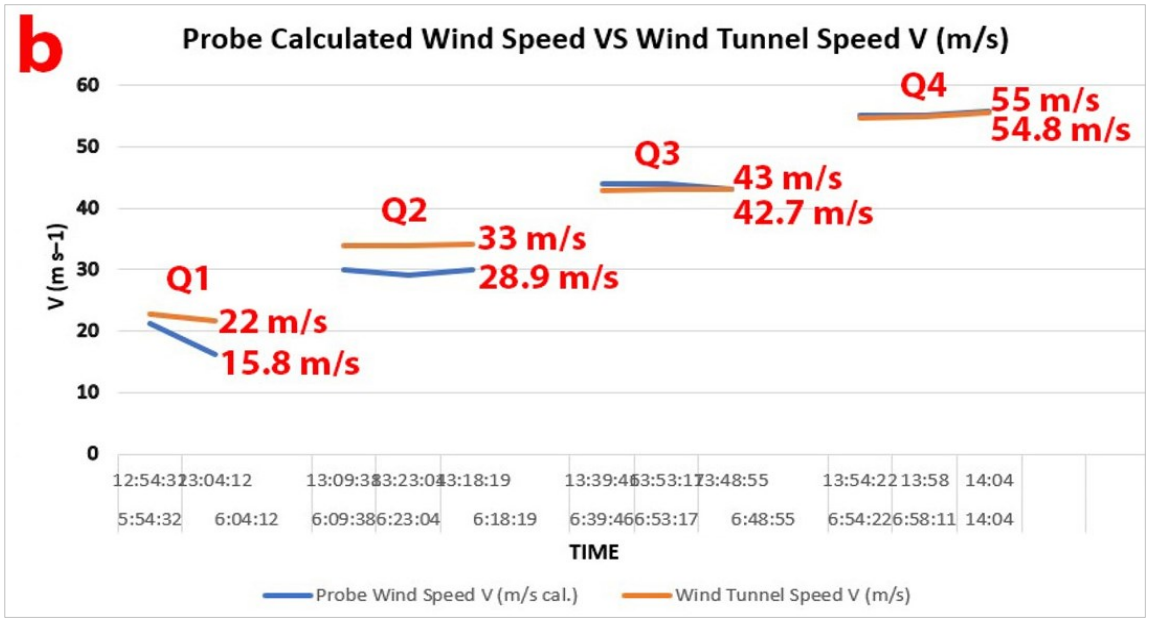

Figure 5: a) Wind-tunnel pressure (P atm) and error rate comparison test results for each Q (applied windspeed) between the INPAR and pressure sensor (raw values) and the wind-tunnel data from start to end of test. Probe raw data (grey line). Each Q highlighted by color code (22 m s^{-1} = blue, 33 m s^{-1} = yellow, 43 m s^{-1} = green, 55 m s^{-1} = red). Bottom left inset shows the wind tunnel and probe start and end of testing data. Bottom right shows average error rate in hPa, b) INPAR calculated windspeed versus wind-tunnel actual speed through each Q (applied windspeed in the wind tunnel). Blue lines are probe-calculated windspeeds; orange lines are wind-tunnel-applied windspeeds. Windspeed differences noted in red in m s^{-1}.

Additionally, wind-tunnel and INPAR comparisons at the start and end of testing revealed even smaller variations in measured pressure with a total of <2-hPa difference. Probe-calculated windspeed versus actual wind-tunnel windspeed are shown in Fig. 5b through each respective Q (applied windspeed within the wind tunnel) and show nearly 7 m s^{-1} difference at the 22 m s^{-1} Q, nearly 5 m s^{-1} difference at the 33 m s^{-1} Q, and <2 m s^{-1} at the 43 m s^{-1} Q. Finally, the difference at the 55 m s^{-1} Q was found to be <0.2 m s^{-1}, indicating that the INPAR calculated windspeed accuracy increased as the windspeed increased (similar to Samaras and Lee 2004), and was nearly identical to the actual applied wind tunnel windspeed, starting near 40–43 m s^{-1} through 55 m s^{-1}.

Hence, the INPAR and BME280 pressure sensor were found to be highly accurate, and comparable to the Samaras and Lee (2004, hereafter SL04) research, particularly with windspeeds >40 m s^{-1}, as highlighted in Fig. 5b.

4. Probe operating principle

Data from the wind-tunnel tests, as seen in Fig. 5(a, b), shows that due to the conical shape and size of the INPAR probes, they can accurately measure the static pressure in high wind environments such as near and inside tornado cores, with the INPAR probe accuracy increasing as the windspeed increases (Fig. 5b). This is achieved via the aerodynamic shape of the INPAR, as detailed in DMH22, which allows the free-stream static pressure to be measured across the entire body of the probe. Because the Samaras HITPR had a proven in-situ observational track record (e.g., SL04; Samaras 2006; Karstens et al. 2010), DMH22 2015 fabrication upgrades included pressure port locations that utilized the SL04 XL and pressure coefficient (C_p) descriptions (Fig. 2a,b), with similar but not matching port locations as the Samaras HITPR (review of the C_p and XL descriptions can found in SL04). Thus, the INPAR Cp calculations and subsequent C_p zero (C_p=0) location (Fig. 2) should also be similar but not exact to SL04. To validate the INPAR compared to the SL04 HITPR findings, the INPAR probe underwent full calibration and validation tests in a wind tunnel, as described above. C_p calculations were completed for the various 22–55 m s^{-1} wind velocities using the SL04 adapted C_p equation [Eq. (1) in SL04] and defined in this study as Eq. (3):

$$Cp = \frac{Pm - Ps}{0.5pV^2} \quad (3)$$

Where: P_m = measured pressure, P_s = static pressure, pV = air density, and V = velocity.

Similar to the SL04 findings, the INPAR wind-tunnel tests showed the C_p variations through the wind axis at an immeasurable distance from the front of the probe (wind-facing side) toward the back of the probe (opposite side) (Fig. 2a). Review of the INPAR X/L length, height, width, and weight dimensions can be found in DMH22. SL04 defined this immeasurable distance as the "X/L" distance, and this study will follow that SL04 naming convention for clarity. While the wind-tunnel velocities applied to the INPAR body were measured under different azimuthal angles (θ) and different radii (r), the results show that when the C_p is at or very near 0 at 0° (i.e., directly facing the wind), the pressure at that surface location [X (Fig. 2a)] is equal to the free-stream static pressure, as can be calculated in the adapted SL04 Eq. (3)., providing a measuring location point [X (Fig. 2a)] where C_p=0 and the surface pressure is equal to the free-stream static pressure. The precise position on the INPAR body where C_p was nearest C_p=0 (shown as the X line point in Fig. 2 a) was found by calculating the C_p measurements for the entire body of the INPAR.

The INPAR wind-tunnel test results were similar but not exact to SL04, showing that the C_p variations at the front portion of the probe (wind-facing side) reduced continuously from between 0.8–0.9 while moving towards the rear of the probe body (opposite side) with the C_p X/L average found at X/L≈0.38 (Fig. 6a), with a thin type boundary layer. Depending on the exact air density, the INPAR C_p nearest C_p=0 was found at 0.03–0.1 (Fig 6b) at 0° (directly facing the wind). Minimum windspeed where the C_p was independent of X/L occurred near 40–43 m s^{-1} while windspeeds near 22 m s^{-1} were largely shifted, as visualized in Fig. 5b and further seen in Fig. 6a.

Akin to SL04, the C_p angular dependence furnished a way of estimating the wind direction and speed. C_p variations at the test angles around the INPAR with a port radius of 13 cm are seen in Fig. 6b. Due to the C_p being negative in all directions around the INPAR, Fig. 6b highlights the negative C_p and shows that at 0° (directly facing the wind), C_p0 is at 0.1 with a

windspeed of 43.75 m s^{-1}. Thus, the radial axis pattern in Fig. 6b shows that when $C_p \approx 0$ directly facing the wind, the pressure is equal to the free-stream static pressure.

Similar to the SL04 findings, INPAR probe wind-tunnel test also found that as the angle increased, Cp reached a somewhat skewed minimum/maximum between roughly 75–80° (Fig. 6b). While the Fig. 6b radial plot appears smaller and jagged from roughly 30°–70°, with smaller angular variations than SL04 (their Figs. 8, 9), concentration at 0° (directly facing the wind), show almost identical but not exact values as SL04 literature. Although the INPAR angular variations are not as strong as the SL04 findings, likely due to the fabrication and placement of the camera shadowboxes on the outside of the probe body, INPAR wind-tunnel data shows moderate to strong C_p variations across the INPAR body and pressure ports at a radius of 13 cm. Because the pressure is the

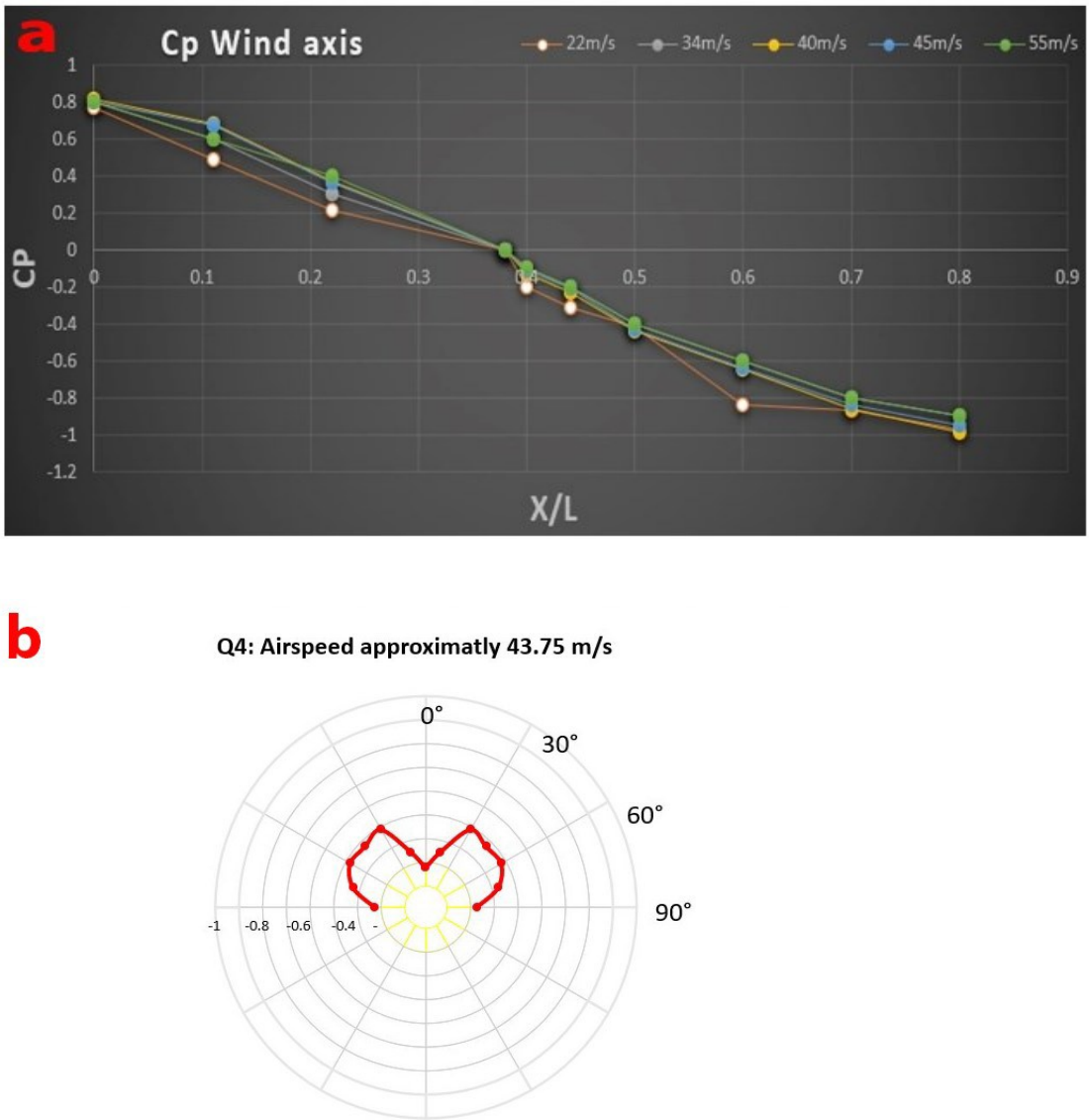

Figure 6: a) INPAR pressure coefficient (C_p) variations in the wind axis (from 22–55 m s^{-1}) on the leading edge from the front of the probe (wind-facing side) towards the back side (rear–opposite side) of the probe showing C_p XL average of 0.38 at 0° (directly facing the wind), b) INPAR wind-tunnel results showing C_p nearest C_p=0 at 0.1 at 0° (directly facing the wind/wind-facing side) with a windspeed at 43.75 m s^{-1} and 13-cm port radius.

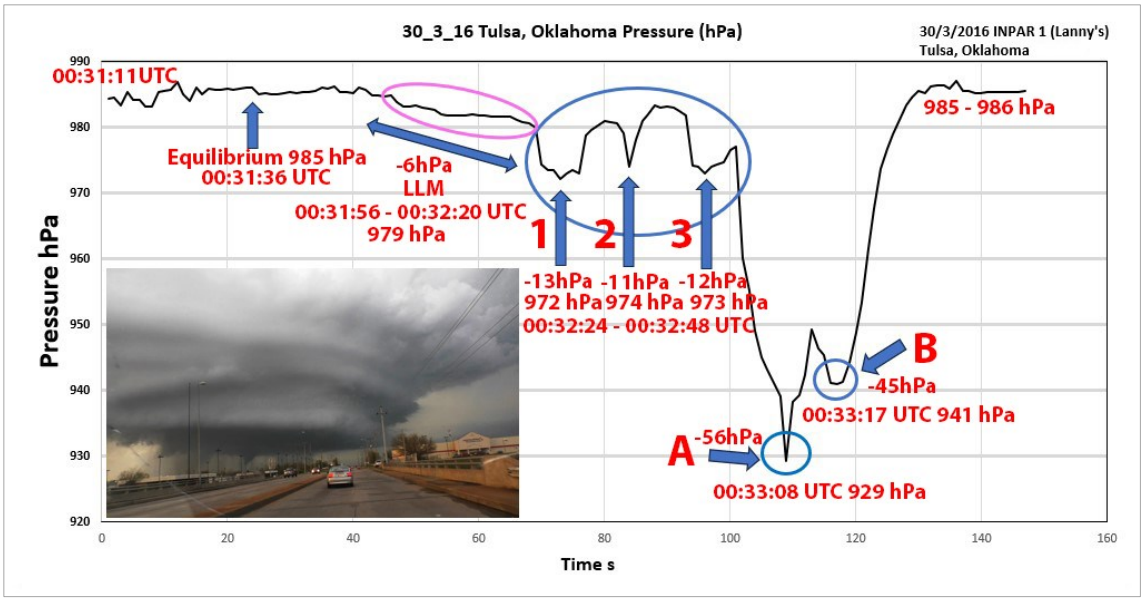

Figure 7: Tulsa, OK near-surface INPAR pressure trace from 00:31:11 to ≈00:35 UTC on 30 March 2016. Timing of equilibrium noted in red near 985 hPa. Pink oval with blue arrow underneath denotes possible LLM –6-hPa deficit. Large blue circle with three vertical blue arrows below labeled 1, 2, 3 shows three pressure dips (–13 hPa, –11 hPa, and –12 hPa) with UTC timing of each dip in red. Large pressure drop highlighted in the first small blue circle with letter (A) shows the main/first Tulsa tornado impacting the INPAR probe with a maximum 56-hPa pressure-deficit. Letter B shows a second 45-hPa pressure drop (second small blue circle) impacting the probe ≈8 s after the main/first tornado. Subset picture in the bottom left shows a picture of the Tulsa supercell and tornado roughly 8 min before probe deployment. View is looking north/northwest. Picture by L. Dean.

highest/lowest in the direction directly facing the wind (i.e., 0° seen in Fig. 6b), the pressure port measuring the highest/lowest pressure is the port the wind is coming from (i.e., the direction the wind is blowing). Identical to SL04, once the direction of the wind is known, the static free-stream pressure is also known. Using the SL04 adapted windspeed equation, Eq. (4), the windspeed then can be found by calculating the measured pressure at a known angle within the wind axis as:

$$V = \sqrt{\frac{2(P_{m\vartheta} - P_s)}{\rho C_{p\theta}}} \qquad (4)$$

Where $P_{m\theta}$ = measured pressure (other than 0°), P_s = free-stream static pressure, ρ = air density, $C_{p\theta}$ is the pressure coefficient at angle θ (other than 0°).

Hence, the pressure at two separate angles around the INPAR can be calculated for the general estimated windspeed. Results from the INPAR C_p and X/L wind-tunnel test are very comparable to the SL04 literature, which found the Samaras HITPR X/L at X/L≈0.3 at C_p=0–0.1. The minor differences between the Samaras HITPR and the INPAR X/L and C_p values are likely due in part to the increased Reynolds number from the shadowbox camera mounts being located on the outside of the probe body, and the flat-top design of the INPAR (described in DMH22) causing slight shifting of the overall flow field.

5. Case events

a. 30 March 2016, Tulsa, OK

The first successful in-situ deployment after the DHM22 upgrades (i.e., post-2015) occurred on 30 March 2016, as the first author activated and deployed an INPAR probe ahead of a fully developed tornado (hereafter Tulsa tornado) in northern Tulsa County, OK, roughly 1.5 mi (2.4 km) northeast of the Tulsa International Airport. The INPAR probe was deployed near or within the forward flank convergence boundary of the Tulsa supercell but still close to the edge of the inflow region, directly ahead of

the approaching Tulsa tornado (Fig. 7 subset picture). After deploying the INPAR, the first author quickly retreated south, awaiting the tornado's passage. The INPAR probe was directly impacted by the Tulsa EF2 tornado, with maximum estimated peak winds of 110–120 mph (49–54 m s^{-1}) by the NWS in Tulsa (NWS 2016).

INPAR in-situ pressure-deficit observations from the Tulsa tornado reveal a fascinating pressure trace, showing the probe reached equilibrium roughly 25–30 s after deployment, near 0031:36, and remained steady near 985 hPa for roughly 25 s. From near 0031:56 through 0032:20 (46 s through 69 s), the pressure slowly decreased roughly 6 hPa to near 979 hPa. Between 71–101 s, the pressure is seen falling and rising multiple times with –13-hPa (972 hPa), –11 -hPa (974 hPa), and –12-hPa (973 hPa) deficits noted from 0032:24 through 0032:48. Between each of these three pressure drops, the pressure would rise quickly before sharply dropping again (Fig. 7). The total time between each pressure drop ranged from roughly 6 s to 2 s. At ≈109 s the pressure substantially dropped to 929 hPa near 0033:08. After 109 s, the pressure then rose through 113 s to 948 hPa, and then sharply dropped to 940 hPa at 0033:17 (118 s). The pressure then quickly rose again to between 985 and 986 hPa by 138 s, where it remained hovering until the first author retrieved the probe. At equilibrium, the pressure was noted at 985 hPa, with the largest measured pressure deficit noted at 929 hPa. The maximum pressure deficit was 56 hPa, with a second deficit maximum of 45 hPa at 0033:17.

The slow 6-hPa drop in pressure from 0031:56–0032:20 is likely due in part to the LLM getting close to or even directly above the INPAR probe. The authors cannot say with certainty that the three spikes in pressure from 0032:24–0032:48 are associated with or directly attributed to the LLM, however. While the Tulsa in-situ deployment was initially intended for testing of the post-2015 DMH22 upgrades, results of the Tulsa pressure data (Fig. 7) revealed interesting characteristics that strongly resemble the Wurman and Samaras (2004) Stratford, TX, pressure trace on 15 May 2003, also characterized by multiple smaller V-shape or U-shaped signatures before and just after the large V-shape signature associated with the Stratford tornado core (discussed further in section 6). Visual observations show the Tulsa tornado was an MVMC (multiple vortex mesocyclone, Wurman et al. 2014), with subvortices extending well outside the parent tornado core region (not shown). While it is unknown if the three pressure-deficit fluctuations seen before the large 56-hPa and 45-hPa deficits (associated with the Tulsa tornado core) are manifestations of one or more of these subvortices impacting the INPAR, it seems a more reasonable possibility than quick pressure-deficit succession caused by the LLM. However, another argument could be made that these three pressure spikes could be related to or a part of the possible O17 VVS. The deployment of the probe within or on the edge of the front flank, near or just behind the FFDB, as the Tulsa tornado was moving toward the probe, also could support a VVS region flowing near the INPAR at the time of documentation, possibly implying three independent VVS vortices (e.g., S13; G18).

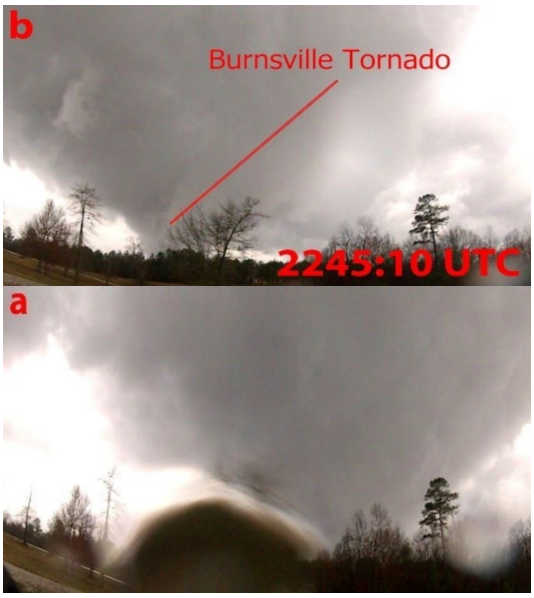

Figure 8: a) Burnsville deployment location 1 video on 23 February 2019, b) Burnsville reposition video with first view of the Burnsville, MS tornado looking south from the deployment 1 location. *Click links to play and enlarge.*

The large 56-hPa maximum pressure deficit certainl is due to the Tulsa main tornado core. Less certain is the secondary 46-hPa pressure maximum, ≈8 s after the Tulsa main tornado core (≤10-s duration) impacted the INPAR. The secondary pressure maxima is likely the INPAR probe's sampling a subvortex. Wurman and Samaras (2004) found two additional pressure

deficit fluctuations during and moments after the Stratford, TX main tornado core impacted the HITPR, and attributed these deficits to secondary or even possible tertiary vortices just after the main tornado. This suggests that the INPAR can distinguish some types of vortex structure within a tornado. Regardless, the Tulsa pressure data demonstrated the post-2015 DMH22 upgrades could resolve pressure deficits adequately in situ, and possibly distinguish vortex structure under the right circumstances. The Tulsa pressure data with a full radar analysis will be provided in a future publication.

b. 23 February 2019, Burnsville, MS

On 23 February 2019, the PACRITEX research team deployed an INPAR probe at 2234:26 UTC (hereinafter all times are UTC), roughly 3 miles (5 km) northwest of Burnsville, MS (Fig. 8a Burnsville deployment location 1 video). The location (34.8510 –88.5336) offered a broken view of the approaching supercell (hereafter Burnsville supercell) to the southwest of the research team location. By 2245:10, the research team caught view of the approaching Burnsville tornado to their southwest and immediately loaded up the INPAR to reposition (Fig. 8b Burnsville reposition video).

Leaving the deployment 1 location near 2245:27, the research team turned right on Highway 72 and continued east through the slenderest part of the hook echo (e.g., Brooks 1949; Stout and Huff 1953; Van Tassel 1955; Fujita 1958). However, due to a limited road network, and because Highway 72 turned in a southeast direction toward Burnsville, this navigational strategy placed the PACRITEX research team directly north and ahead of, but eventually crossing the projected path of, the northeastward-moving Burnsville tornado. Because the Burnsville tornado was initially highly visible (Fig. 8b), the researchers felt confident in continuing deployment attempts.

Disclaimer: *What follows is a detailed description of a potentially dangerous situation of a subsequent deployment. Importantly, note that the Burnsville case in this study describes in-situ video with detailed first-person observations from experienced storm researchers in an extremely dangerous situation, with root causes extending back to navigational strategy, lack of road network, false sense of visibility, and injury, all of which contributed to being inadvertently struck by the Burnsville tornado. The authors want to make it abundantly clear that the actions described here are inherently dangerous and should not be attempted unless extremely experienced. Even then, there is a potentially fatal level of risk associated with this data collection effort. While the authors do not condone intentionally being in such a perilous situation, we believe that the audience could benefit greatly from the viewing of these in-situ videos as what not to do, or what could happen, while the storm-research community could benefit by possibly using these detailed observations as a reference for further research. Additionally, a few of the scientific video observations described in this study show one PACRITEX team member within the in-situ video. This was not intentional and is due only to the direction the probe cameras were pointed, capturing the scientific features of interest. However, due to obvious ethical concerns, only one in-situ video figure showing a team member near and within the damaging inflow and tornado core regions is highlighted in this study. The remaining in-situ videos have been placed in the text and Appendix as external links.*

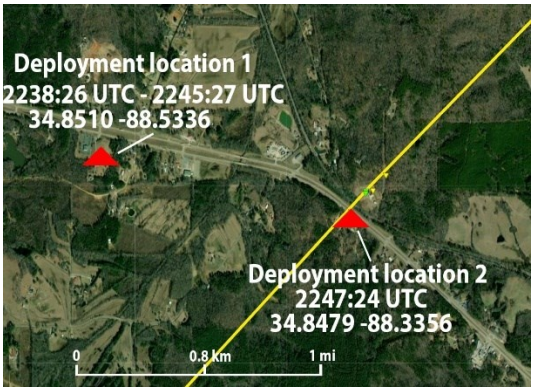

Figure 9: INPAR probe deployment locations (red triangles) with time and GPS locations. Yellow line denotes Burnsville, MS tornado path. Green and yellow triangles show damage rating. Background image courtesy NOAA Damage Assessment Toolkit. *Click to enlarge*.

During transit toward the second Burnsville deployment location, the research team briefly but clearly saw the Burnsville tornado to their immediate south, but quickly lost view due to terrain features and increasing precipitation. By 2246:15, the team's rate of travel slowed considerably, as they experienced strong easterly inflow winds but decreasing precipitation. The

team likely crossed the LFCB, followed by the FFCB, as they traveled eastward on Highway 72, resulting in less precipitation and providing the researchers with a false sense of visibility. Probe video analysis near 2246:50 shows the research team pulled to the shoulder of Highway 72, near Lake Drive (34.8479 –88.3356), to attempt a second deployment (Fig. 9). The inflow jet increased in strength, damaging a house 62 m west of the research team (Appendix, Burnsville inflow video 1). Near 2246:55, a PACRITEX team member and the third author of this study (RH) partially pulled the INPAR from the rear of the vehicle, attempting to continue the second deployment. Near 2247 UTC, probe-based video observations show a brief view of an interesting feature that can be described as a small rotating bowl-shaped lowering descending and moving westerly along Highway 72 (Fig. 10, Burnsville bowl lowering video).

Figure 10: Probe video screen capture of the Burnsville bowl lowering near 2247:01 UTC. Probe view is looking west. Contrast and tone slightly enhanced to show the bowl lowering feature better. *Click link to play video and enlarge*.

While the Burnsville bowl feature meets the Glossary of Meteorology's definition and criteria of a funnel cloud [Funnel cloud—Glossary of Meteorology (ametsoc.org)] in that it was rotating aloft with no discernable ground contact, the bowl lowering was displaced roughly 100–200 m (328–650ft) to the northeast and ahead (i.e., in front) of the tornado and associated inflow jet, near the FFCB/FFDB, and near where the possible O18 SVC edge and PDL locations might be, as highlighted in the O17 and O18 simulations. Although view of the bowl feature is brief, independent video analysis and first-person observations from the research team show the bowl feature was rotating cyclonically and widening while visually descending. At the same time, the front bottom portion of the bowl appeared to arch out and then curl back or, rather, fold in upon itself (i.e., the right front portion closest to the ground curling inwards towards its base). By 2247:05, a slight fall, followed by a brief rise, is noted in the pressure trace (discussed below). This brief pressure perturbation is nearly consistent in time and location, with the bowl feature passing very near or directly over the research team.

Although it is not known what percentages of supercells have an SVC, or if the Burnsville supercell had an SVC, due to the bowl feature moving toward the Burnsville tornado, the Burnsville bowl lowering attribute could be a visual manifestation of a possible VVS vortex moving along, or between the edge of the possible VVS (e.g., O17), and the inflow channel (e.g., Broyles et al. 2022). This is due in part to the pressure gradient caused by the possible helical SVC being tilted from the horizontal into the vertical, near the LLM and tornado core. (e.g., O18). However, another reasonable argument is that the Burnsville bowl feature is simply a funnel cloud or a secondary circulation possibly associated with an LLM/tornado cycling or occlusion phase independent of the Burnsville tornado and immediate inflow layer. This possibility is similar to Houser et al. (2015, hereafter H15) mobile-radar observations of dual LLMs and dual tornadoes during the 24 May 2011 El Reno, OK tornado, which they described as neither the dual mesocyclones or tornadoes evolving "in a manner entirely consistent with any published conceptual model of supercell cycling, although certain aspects were similar to classic conceptual models."

Usually, when two mesocyclones are ongoing within a single supercell, it is part of the overall cycling process of the supercell. As the old mesocyclone occludes, the new mesocyclone further develops and or strengthens (e.g., Lemon and Doswell 1979; Burgess et al. 1982; Dowell and Bluestein 2002). Under the right conditions, this cyclic mesocyclogenesis (e.g., Adlerman et al. 1999; Adlerman and Droegemeier 2002) could increase the potential for a new tornado, as seen in Davies et al. (1994), Wakimoto et al. (1998), and Wurman and Kosiba (2013). LLM and tornado cycling with occlusions can and do occur with multiple ongoing tornadoes (e.g., Davies et al. 1994; H15) nearly ongoing tornadoes simultaneously (e.g., Wienhoff et al. 2020; Wurman and Kosiba 2013) or even multiple LLM's within a single supercell, as observed by Boustead and Schumacher (2008) and H15.

Previous mesocyclogenesis simulations (e.g., Adlerman et. 1999; Adlerman and Droegemeier 2002; 2005) show two basic mesocyclogensis modes: i) the occluding cyclic mesocyclone mode (OCM) and ii) the non-occluding cyclic mesocyclone mode (NOCM), both supported by field observations (e.g., Dowell and Bluestein 2002; French et al. 2008; H15). Although independent video analysis revealed the Burnsville bowl lowering was moving from east to west, the bowl feature's location seems consistent with the Burgess et al. (1982) cyclic mesocyclogensis conceptual model. Assuming the bowl feature was associated with an OCM or NOCM, as described by Adlerman and Droegemeier (2002; 2005), the Burnsville bowl lowering may be part of a cycling occlusion (e.g., Wakimoto et al. 1998; Beck et al. 2006; French et al. 2008; Boustead and Schumacher 2008; Kumjian et al. 2010; Wurman and Kosiba 2013; Skinner et al. 2014; H15; Wienhoff et al. 2020), or perhaps merging or handoff type phases, as described in Davies et al. (1994).

To verify possible LLM cycling and occlusions near or just before the bowl lowering observations that could be related to the bowl feature, dual-polarization (dual-pol) radar analysis using the Columbus Air Force Base (KGWX) WRS-88D were completed. While two distinct mid-LLMs were found near 2241 UTC, one roughly 3 mi (4.8 km) northwest of Burnsville, and the second roughly 4 mi (6.4 km) southwest of Burnsville (not shown), the Burnsville supercell was roughly 55–60 nm (102–111 km) away from KGWX with 0.5°-elevation beam heights ranging from 4900–6200kft+ (1.5–2 km) ARL from 2241–2247 UTC. Thus, LLM genesis that could affect low-level features like the Burnsville bowl lowering is likely not readily identifiable due to low-quality radar returns. Because the KGWX analysis from near the time of the bowl lowering, just before 2247 through in-situ impact, does not show quality, valuable near-surface low-level radar features that could be associated with the bowl lowering, the authors have little confidence suggesting the bowl lowering was definitively associated with an LLM cycling phase. That is not to say that an attempted LLM and tornado cycling phase did not occur, but rather, the authors did not visually observe a cycle or occlusion phase. Insufficient quality low-level radar data is apparent to show otherwise. While this feature possibly was associated with a new mesocyclone in a manner like the cycling process, its association with a VVS vortex cannot be ruled out.

The Burnsville bowl feature was located some distance ahead and independent of the Burnsville tornado, and was not a satellite vortex of the Burnsville tornado as defined in Edwards and Dean (2018), nor an MVMC circulation (Wurman and Kosiba 2013), or even a subvortex as seen in DMH22. As such, the bowl lowering could be a VVS vortex not in visible contact with the ground. The movement and location of the bowl feature in relation to the Burnsville tornado, as well as the brief pressure deficit, correlates well with the O17, O18, and Orf (2020, hereafter O20) simulations of a possible VVS misovortex moving toward the Burnsville tornado. Additionally, F18 and F23 highlight multiple rivers of vorticity surges and even individual vertical vortices within each surge of the possible VVS flowing back towards the updraft-downdraft interface, throughout the life cycle of their simulation of an EF5 tornado from the 27 April 2011 outbreak, possibly like the S13 and Griffin et al. (2018) LRR radar observations.

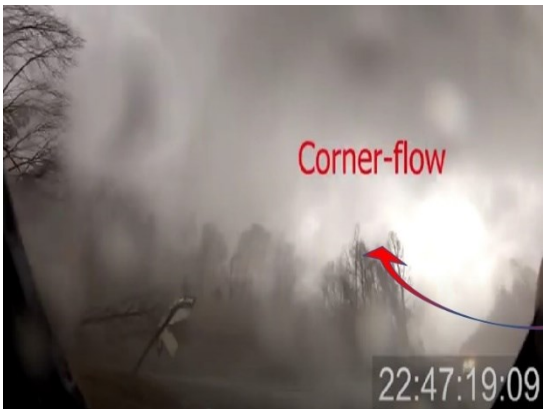

Figure 11: Probe video screen capture of the Burnsville corner flow video starting at 2247:18 UTC on 23 February 2019. Red arrow denotes inflow with view looking west. *Click link to play and enlarge.*

Near 2247:19, INPAR probe video shows a unique and seldom documented feature just to the west of the research team. The Burnsville tornado inflow was manifested by low-level condensation racing westerly into the corner-flow region and rapidly rising into the eastern edge of the tornado core. Near 2247:19:09, the corner-flow region became clearly visible roughly 70–80 m west of the research team as the immediate tornado inflow continued, as seen in Fig. 11.

Study of the Burnsville tornado inflow is important in that there are few in-situ and visual observations, much less first-person observations, describing the inflow characteristics near the corner-flow region [(i.e., that region where the tornado core meets the surface and the immediate inflow, where the mostly horizontal flow is abruptly tilted into the vertical) (e.g., Lewellen (1976)]. Rightfully so, this corner region is where the most damage in tornadoes likely occurs due to a number of factors, including possible significant pressure deficits, some near or exceeding 100 hPa (Lee et al. 2004; Blair et al. 2008). The obvious dangers faced by researchers while attempting to sample or observe the immediate inflow or corner regions in situ make them exceedingly hard to obtain due to high wind velocities, low visibility, poor road network and conditions, and erratic vortex behavior, all of which could lead to being impacted by the tornado (as this study shows).

While simulation and research work (e.g., Lewellen et al. 1997; Davies-Jones et al. 2001; Xia et al. 2003; Lewellen and Lewellen 2007) and direct boundary-layer observations (e.g., Bluestein et al. 2014) have helped our understanding of the immediate inflow and corner-flow regions, there are only a limited number of in-situ observations that have documented the immediate tornado inflow at the corner section (described below). This leaves considerable debate as to the processes and possible lowest pressure deficit values that may be attainable within tornado cores, as suggested by Blair et al. (2008).

First-person and probe video observations of the Burnsville corner-flow region near 2247:19:12 (hours, minutes, seconds, frames) show the tornado inflow strengthened, with cloud tags and debris adjoining the corner region from nearly all directions. Near 2247:20:01, a strong northwesterly to northerly inflow jet is manifested by a band of dark cloud tags and debris, flowing northerly to southerly across Highway 72 into the corner-flow region, just behind a vehicle traveling eastward on Highway 72 (i.e., just to the rear of the eastward moving vehicle lights in Burnsville corner flow video). Near 2247:20:10, the Burnsville tornado was still to the southwest of the research team's position, moving northeasterly; however, the research team members visually observed the Burnsville tornado appear to widen, turn (wobble) right, and strengthen almost simultaneously, moments after the northwesterly inflow jet was seen being pulled into the corner-flow region, as it moved along and across Highway 72. This sequence is supported by the NWS damage assessment suggesting the Burnsville tornado intensified through this area (Fig. 9).

By 2247:20, probe video analysis shows heavy and nearly blinding precipitation flowing horizontally back toward the Burnsville tornado core, which was now roughly 20 m west of the research team. The research team likely experienced some portion of either the LFCB or FFCB at the updraft-downdraft interface/tornado core and LFCB and FFCB intersection just before being struck by the Burnsville tornado. At 2247:24, the research team was struck by the right front quadrant of the Burnsville, MS EF2 tornado. Independent video analysis from 2247:21 through 2247:25 shows the research team was not impacted by the strongest part of the tornado (i.e., the tornado core) but rather the right front periphery of the corner-flow region and that the tornado core passed roughly 1–3 m (6–12ft) to their immediate north (Appendix: Burnsville impact 1 video).

Because the primary focus of the PACRITEX 2019 field research campaign was the possible O17 VVS and PDL regions, the analysis of the pressure trace recorded on 23 February 2019 focuses on two specific timeframes: i) near the time of the bowl lowering at 2247 and ii) the impact and passage of the tornado at 2247:24. Figure 12a shows the full recorded pressure trace as a time-series plot starting at 2234:26, continuing through 2254. The Burnsville pressure trace is consistent with previous in-situ pressure deficit documentation (e.g., Karstens et al. 2010; SL04; Blair et al. 2008; Lee et al. 2004; Wurman and Samaras 2004), showing an overall gradual decrease in pressure followed by a large pressure deficit indicative of the tornado passage, and then an abrupt rise in pressure with values returning to near previously recorded values or pre tornado values. Probe activation occurred at 2238:26 from deployment location 1, with the INPAR probe reaching equilibrium with consistent pressure near 990 hPa between 53–99 s (Fig. 12a). A slight downward trend in pressure is seen from roughly 100 s with some fluctuations through 180 s. The authors cannot explain these slight dips and rising fluctuations.

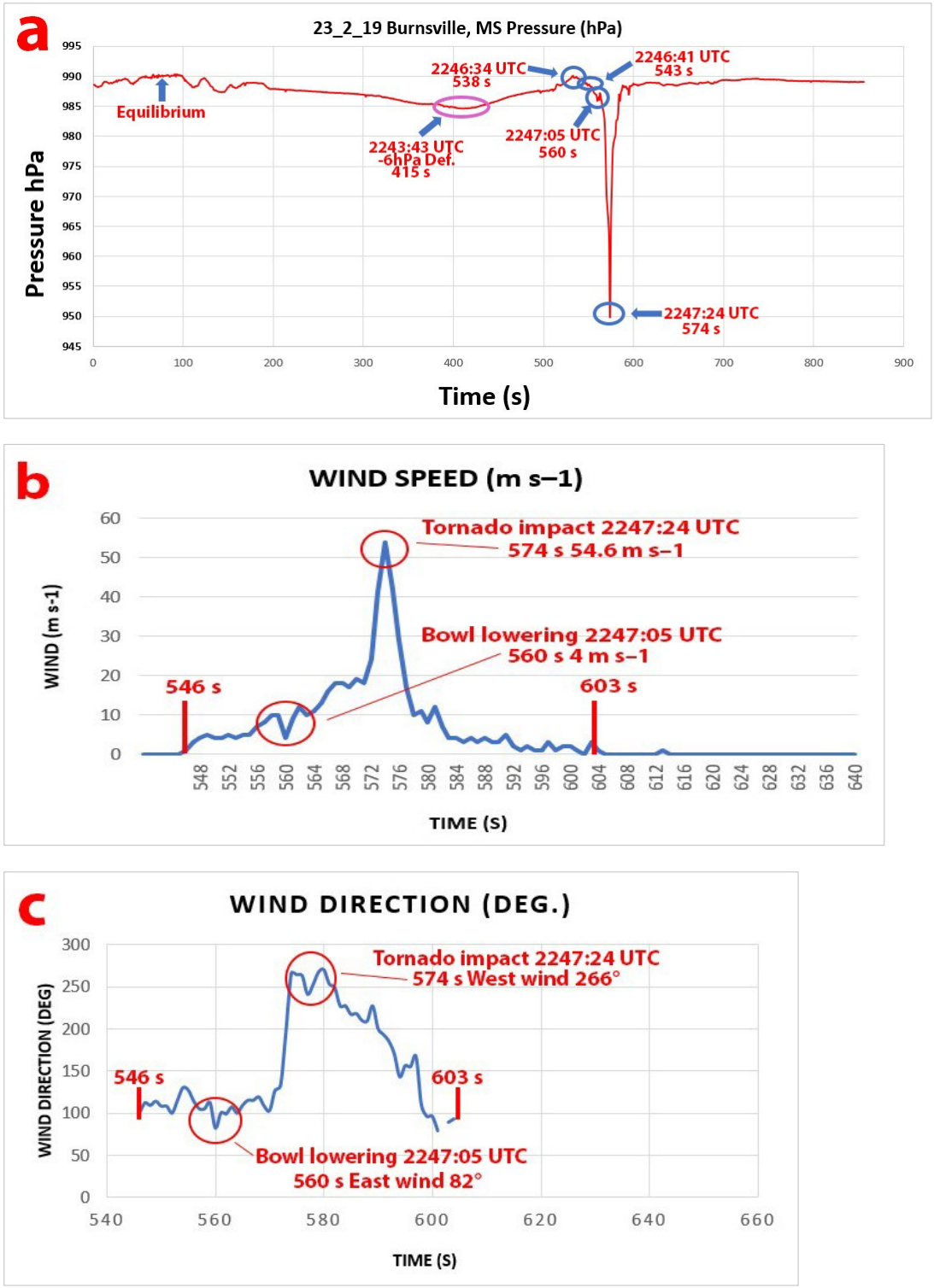

Figure 12: a) Burnsville, MS INPAR pressure trace at 0.61 m (2 ft) AGL from 2234:36 through 2254:00 UTC on 23 February 2019. Timing of equilibrium noted in red, 6-hPa deficit purple oval. Bowl lowering passage (2247:05), and impact and passage of tornado (2247:24) noted in red, b) estimated windspeed observations of the Burnsville tornado on 23 February 2019, c) wind-direction observations of the same tornado. Bowl lowering and tornado impact highlighted in red circles with time UTC.

At 2243:36, gradual decreasing pressure is seen from roughly 195–400 s with a roughly 6-hPa pressure drop to 984 hPa noted by 415 s. This 6-hPa deficit may be due to the Burnsville mesocyclone's getting closer to the research team at the deployment 1 location, or perhaps the INPAR's resolving some portion of the possible O18 PDL. Near 2243:52 (422 s), a gradual rise in pressure is noted, lasting through 2245:30 (492 s), where another fluctuation appears (Fig. 12a). The research team caught their first view of the Burnsville tornado near 2245, where they then loaded up the INPAR to reposition. The small fluctuations near 2245:30 (492 s) are attributed to manually picking up the probe and loading it into the rear of the vehicle, as highlighted in Fig. 8b (Burnsville reposition video) [(and likely also seen on four occasions during the 96-h comparison test (Fig. 4), as first author picked up the probe to verify the battery was working)].

Additionally, the continued gradual rise in pressure noted from 2245:30 (492 s past 543 s, Fig. 12a) coincides with the probe's being inside the vehicle as the research team traveled toward the second deployment. Wind velocity data in Fig. 12b from near and just past 540 s also reflects the INPAR probe's being in the vehicle. Fig. 12c shows the INPAR wind direction measurements during the bowl lowering passage and the Burnsville tornado impacting the PACRITEX research team. Video inferred from the INPAR video cameras during the bowl feature and during the Burnsville tornado are in generally good agreement with the INPAR wind observations (Fig. 12c).

During the second Burnsville deployment, the INPAR probe was exposed to the outside environment between 2246:54–2247:00. Independent probe video analysis during this timeframe shows the Burnsville bowl lowering to the immediate west of the research team, moving west along Highway 72. Pressure-trace characteristics during this timeframe reflect a brief but sharp decrease in pressure through 2247:05 (560 s, Fig. 12a). By 2247:05:10, the probe video view of the bowl feature is lost as deployment attempts continued. Independent video analysis with close pressure trace inspection at 2246:54 through 2247:07 reveals a pressure deficit fluctuation near 2247 (560 s), followed by a quick rise in pressure seen through 2247:07 (562 s, Fig. 12a). This episode of quick pressure fall and rise correlates with the precise time the bowl feature moved very near or directly over the PACRITEX research team near 2247 UTC.

Because the pressure already was falling rapidly before the bowl feature passed the research team and INPAR probe, it was difficult to determine the exact pressure deficit. Before that, the pressure was ≈990 hPa at 2246:34 (538 s). Using the lowest recorded pressure believed to be associated with the bowl feature near 2247:01– 2247:05 (560 s), we find the lowest pressure value of roughly 984 hPa (560 s), nearly correlating with the time the researchers experienced the first ear popping. This event occurred simultaneously with a 4–5-hPa pressure deficit believed to be associated with the passage of the bowl lowering.

From 2247:25 through 2247:45, a quick rise in pressure to nearly 988 hPa is seen in the Burnsville pressure trace, associated with the tornado passage. The pressure then gradually increased, where it leveled off at near 989 hPa through the remainder of the recorded trace (Fig. 12a). At equilibrium, the recorded pressure noted was 990 hPa. This serves as the base environmental pressure for this study. At 2247:24, the pressure depression reached 949 hPa for a total pressure deficit of 41 hPa.

Although quality concerns exist with the Burnsville wind and pressure data (discussed further in section 7), angular pressure measurements on the INPAR facilitated calculating the estimated wind velocity (described in section 3). A peak calculated gust of just over 54 m s–1 (Fig. 12b) at 2247:24 (574 s) corresponded to the precise time the researchers were struck by the Burnsville tornado and the documented 41-hPa pressure deficit (Fig. 12a). While INPAR probe wind direction estimations (Fig. 12c) correlate well with the timing of both the probe-calculated windspeeds (Fig. 12b) and the 41-hPa pressure deficit, there are concerns with these data. Given the issues during the Burnsville deployment (i.e., partial deployment, questionable flow field in and around the probe and vehicle), the Burnsville data presented here are in question as numerous unintended influences could be biasing the observations (described in section 7). As such, the Burnsville observations are presented here for documentation, considered estimates only, and should be used with caution.

c. 17 May 2019, McCook, NE

On 17 May 2019, the PACRITEX research team intercepted a tornado (hereafter McCook tornado) in Red Willow County, NE, roughly 5 mi (8 km) northwest of McCook. The McCook tornado was rated an EF2 with estimated peak winds of 120 mph (54 m s^{-1}) by the National Weather Service in Goodland, KS (May 17th, 2019 Tornadoes (weather.gov). The tornado visually appeared as cone-shaped condensation funnel with a large dust column directly beneath, and was located on the cusp of the RFD clear slot and the edge of a small broken wall/inflow tail cloud (Fig. 13a McCook tornado video 2 FULL). Near 2257 UTC, the research team deployed an INPAR probe in the grass on the west edge of Road 381, roughly 0.25 mi (400 m) south of Road 720. The location [Fig. 13b (40.2631 –100.7051)] offered

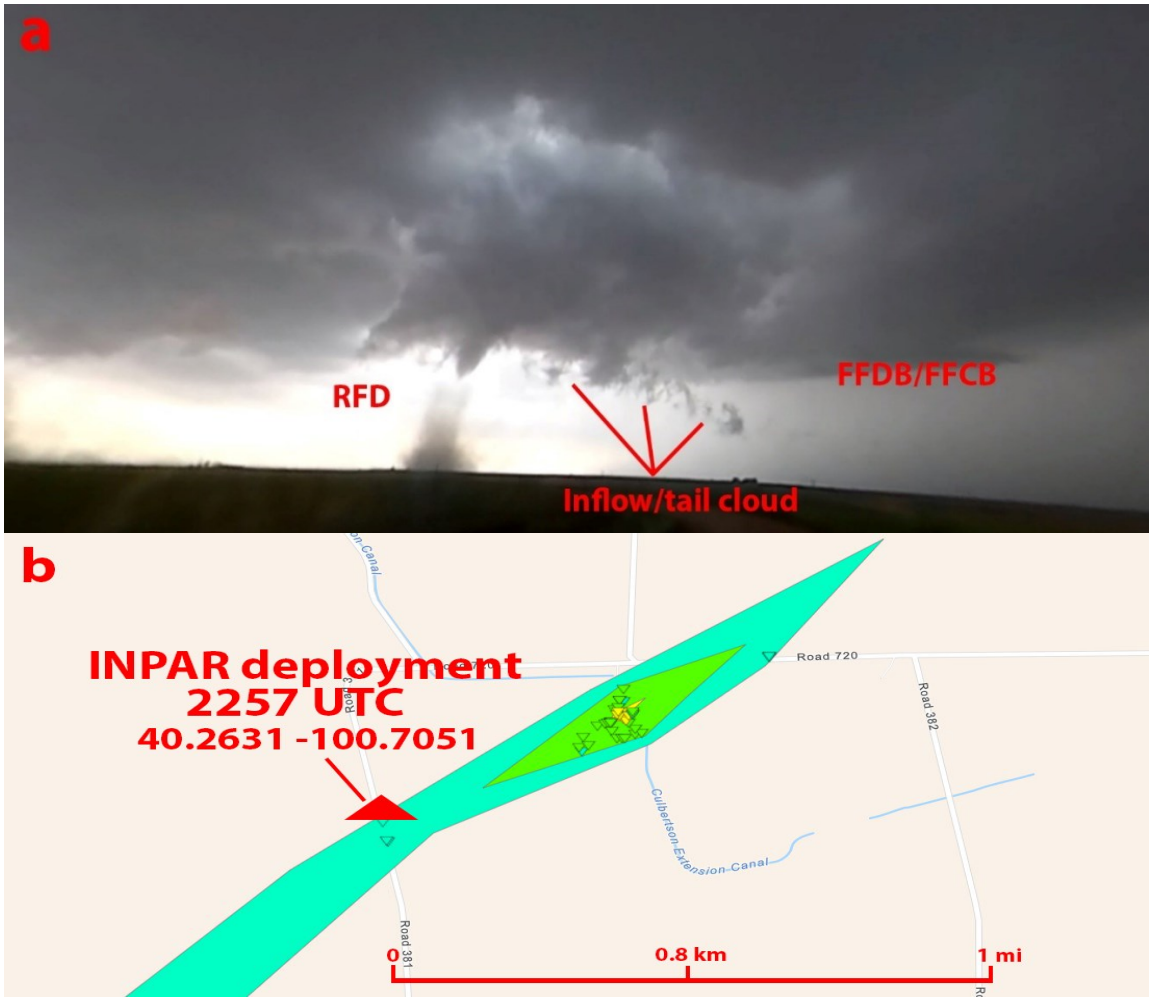

Figure 13: a) Developing McCook, NE tornado (McCook tornado video 2 FULL) with RFD clear slot, broken tail cloud, and FFCB/FFDB noted in red. View is looking west from Road 720, b) McCook, NE deployment location of the INPAR probe at 2257 UTC. Red triangle denotes the INPAR probe location. Background image courtesy NOAA Damage Assessment Toolkit.

an unobstructed view of the northeastward-moving tornado. By then, the tornado had condensed fully to the ground and visually appeared as a slender cone with a large dust plume ahead of and directly under the tornado.

While the dust plume prevented a view of the corner-flow and tornado core regions, probe video and video from the research team show that the McCook tornado was likely a single-cell vortex that appeared to "kink out" in an easterly direction just below the cloud base, near the

LCL. This kink visually appeared to slow the forward speed of the McCook tornado and caused the core to shift south, west of Road 381, roughly 200–300 m southwest of the INPAR probe between 2257:47 and 2258:47. By 2259:15, probe video observations show the left-front quadrant of the tornado core nearing Road 381, roughly 30–60 m south of the INPAR, with the near in-situ outer winds affecting the probe starting near 2259:23 (±1 min as discussed below). Probe video analysis shows that the tornado core did not impact the probe directly, but rather obliquely side-swiped it, while translating erratically (Fig. 13a McCook tornado video 2 FULL).

Pressure-trace characteristics show that the research team activated the INPAR probe around 2242 UTC, some distance away from the McCook supercell, to verify all electronics were in working order and to allow the probe to reach equilibrium. Near 2257 (620 s), the research team deployed the INPAR probe in the grass on the west side edge of Road 381. Similar to the Burnsville pressure trace, interesting pressure fluctuations occurred ahead (upstream) of the McCook tornado.

Near 2257:10 (630 s), the pressure trace shows an increase to near 904 hPa moments after deployment, decreasing to 900 hPa near 2257:29 (649 s), followed by a quick increase to 902 hPa from near 2257:34 through 2257:42 (654–662 s). The authors believe these first pressure fluctuations are likely due to the probe's attempting to reach equilibrium after being removed from the vehicles ambient temperatures and placed on the side of the road. However, near 2257:42 (662 s), the pressure sharply dropped to 896 hPa by 2258:03 (678 s) and remained hovering between 896 and 900 hPa through 2259 (743 s) (Fig. 14).

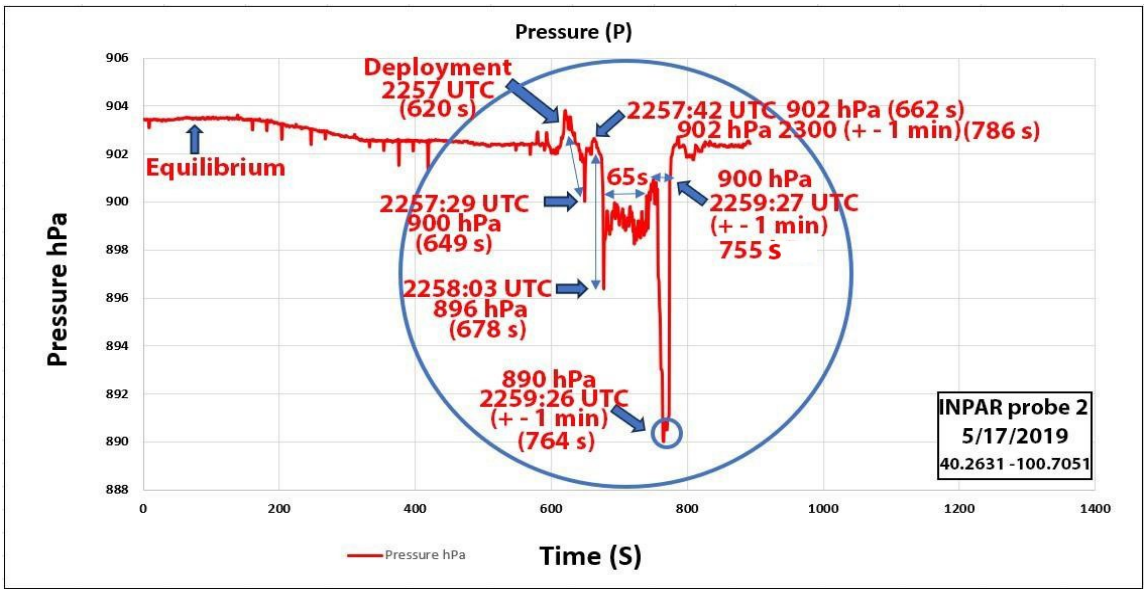

Figure 14: McCook, NE near surface INPAR pressure trace from 2242 through 2303 UTC 17 May 2019. Timing of equilibrium, deployment, and pressure deficits highlighted in red.

Pressure-trace observations show this 6-hPa deficit lasted for ≈65 s before the pressure quickly rose back to near 901 hPa near 2259:09. Near 2259:26 (764s), the pressure-trace timestamps show inaccuracies of roughly 47 s. This issue was caused by increasing the GPS and BME280 sampling rates. To increase the pressure-trace resolution issues of 1 Hz (discussed below), the lead author increased the sampling rate from 1 Hz to 40 Hz (forced mode) of the BME280 and the L80-M39 GPS roughly one month before the McCook tornado. While the GPS timestamps were initially correct until roughly 2259:26, the GPS satellite signal probably was lost between 2259:20 and 2259:26 (765s), and then regained just before 2300. However, enough inconsistencies existed to caution using the exact timing of the probe GPS. Thus, video timestamps were also used after 2259:20 with a ±1 min accuracy through the remainder of the McCook deployment.

Near 2259:22 (±1 min), probe and research team video shows the McCook tornado starting to cross Road 381 roughly 20 m south of the INPAR, with the outer periphery winds impacting the INPAR probe near 2259:23. By 2259:26 (764 s ± 1 min), probe pressure measurements concur with the video observations, dropping from 900–890 hPa (Fig. 14) as the outer tornadic winds obliquely impacted the INPAR probe and the tornado crossed Road 381 (Fig. 13a McCook tornado video 2 FULL). This resulted in a total pressure deficit of ≈13 hPa. The pressure then immediately rose to 902 hPa through 2300 (787 s), indicating tornado passage. The pressure then stabilized at ≈902 hPa through the remainder of the trace (Fig. 14), nearly identical to the pressure observed prior to and immediately following deployment, and before the tornado.

Although the McCook wind data revealed an estimated peak wind velocity near 35 m s^{-1} (not shown), similar to the Burnsville wind data, the authors also question the quality of the McCook wind-data calculations due to the minimum roughly 40 m s^{-1} windspeed where C_p was found to be independent of X/L (described in Section 4). Because the wind-tunnel test results revealed the probe's X/L and C_p dependence decreased as the applied windspeeds increased (Fig. 5b), finding that the minimum windspeed where C_p was independent of X/L occurred near 40–43 m s^{-1} with error results of only 1.7 m s^{-1} at 43 m s^{-1}, and error results <0.2 m s^{-1} at 55 m s^{-1} (Fig. 5b), the authors have skepticism in calculation results with values of less than 43 m s^{-1}. Thus, the authors concern with the angular dependence calculations of the McCook tornado as the outer winds (of roughly 35 m s^{-1}) of the vortex obliquely sideswiped the INPAR probe and did not directly impact it. At any rate, probe wind-direction observations are in good agreement with probe and team video observations during this timeframe.

While there is likely no way to know if the Burnsville supercell had an SVC, the McCook supercell was also observed by the TORUS field campaign for an extended timeframe [TORUS_2019 Field Catalog | NCAR EOL (ucar.edu)]. Those observations revealed an SVC through at least some portion of the McCook supercell lifecycle. In likely one of the most comprehensive studies of the SVC and associated features to date, Satrio (2023) traced parcel trajectories backward and not only found evidence of the SVC (described in Section 1), as highlighted in O17, O18, O20, and f23, but also vorticity budgets showing strengthening of the LLM with parcels that originated within the forward-flank region (i.e., along and behind the FFDB/FFCB). Thus, Satrio (2023) clearly showed the importance of the forward-flank baroclinic generation of streamwise horizontal vorticity during multiple portions of the McCook supercell lifecycle, and that the SVC is legitimately physical.

6. Comparisons and analysis

The symmetrical V shape characteristics of the Tulsa, Burnsville, and McCook pressure traces are similar to others previously recorded. The Burnsville trace appeared similar to the Blair et al. (2008) trace, while the Tulsa and McCook traces show a striking resemblance to that in WS04 for Stratford, TX. Lewis and Perkins (1953) highlighted measured pressure traces from nine separate barographs obtained during a tornado on 8 June 1953 in Cleveland, OH. The barographs ranged from 720–2300ft (219–701 m) from the tornado center, each showing a similar symmetrical V shape. Eight of nine Lewis and Perkins barographs also show large pressure-deficit fluctuations, followed by a brief increase in pressure before the main pressure deficit associated with the tornado occurred (their Fig. 3).

Similarly, at least six of the Karstens et al. (2010, hereafter K10) pressure traces recorded during nine separate TWSTEX deployments appear to have a similar quick drop in pressure, followed by a brief rise or even multiple fluctuations, sometimes lasting only seconds before the main tornado pressure deficit (their Fig. 7 a–f). The K10 pressure profiles also show that most of their observations, including those from the mobile mesonets (MM), were obtained ahead of or from a mostly upstream position with respect to the tornado's direction of travel. Additionally, two of the K10 observations specifically mention pressure fluctuations noted from various upstream positions, which were thought to be related to weaker subvortices, as described in Lewellen et al. (1997).

The Blair et al. (2008) in-situ observations during the 21 April 2007 Tulia, TX tornado event also reveal a small brief pressure deficit near 00:54:50, then a brief rise at roughly 00:54:53 (their Fig. 11), followed by the 194-hPa pressure drop associated with the Tulia tornado

core impacting the observers. While smaller brief pressure fluctuations, like those seen in the Tulia pressure trace, are usually attributed to smaller-scale vortices (Orf 2023, personal communication), Blair et al. (2008) specifically highlight the Tulia tornado as a single-cell vortex before and as the observers were struck, noting subsidiary vortices only after being impacted by the Tulia tornado (their Fig. 8). Thus, their argument was for corner-flow collapse just as they were struck.

Another possibility for these brief pre-tornado pressure fluctuations could be the LLM surface pressure falls, or what Karstens et al. (2010) referred to as the cascading of vortices. While this seems an appealing way to explain these pre-tornado pressure deficits, more reasonably the LLM surface pressure fall would take longer to pass over simply due to the size of the LLM. Hence, a longer drawn-out pressure trace, possibly like Tulsa and Burnsville 5–6-hPa pressure deficits prior to the tornado core. Another sensible argument could be made that the brief pressure fluctuation noted in the Tulia trace, between 00:54:50–00:54:53, could be attributed to a vortex within the possible VVS flowing towards the Tulia tornado/LLM from northerly to southerly (e.g., S13; Kosiba et al. 2013; G18; F23). The Blair et al. wind data (their Figs. 9, 10, 12, 16) and occupant observations support being in a possible O17 southerly flowing VVS, as it flowed back toward the Tulia LLM/tornado core (e.g., Fig. 7 in O17).

While some contention exists surrounding the Blair et al. (2008) 194-hPa pressure deficit with respect to vehicle movement, possible equipment issues, and other related concerns (K10), the Blair et al. (2008) research shows the observers were located upstream (in the path) of the Tulia tornado before, and during the tornado impact (their Fig. 18). This location, as highlighted in O17, O18, and F23, certainly would have experienced the possible VVS flow, if one were present, due to the Tulia tornado still being in the early maintenance phase (e.g., O20), and could have sampled some portion of the possible O18 PDL prior to the tornado core's impact. Moreover, the authors question if the Blair et al. proposed record-setting 194-hPa deficit might be associated with, or even a direct result of, a possible VVS vortex in concert with the corner-flow collapse as an additional reason for such an extreme low-pressure value. The authors agree with Blair et al. that their position was left of center of the Tulia vortex, which also establishes their position relative to the possible VVS region, flowing around and into the LLM and tornado core (e.g., S13; G18; F18; F23).

Research from W99 acknowledged a pressure rise or spike seen during the Allison, TX F4 tornado on 8 June 1995 (their Fig. 11), but suggested that it may be associated with the "ring of high pressure surrounding the central low pressure" of the tornado, as discussed by Ward (1972). The Burnsville and McCook pressure traces also contain pressure rises similar to the W99, seen in Fig. 12a near 2246:34 (538 s) and Fig. 14 at 2257:42 (662 s), and likely in the Manchester, SD pressure trace (Fig. 21 in Lee et al. 2004), but not the Tulsa trace nor some of the K10 observations. Therefore, it is uncertain if this rise in pressure or "ring of high pressure" is the same as W99.

Although the W99 pressure observations were measured from two separate probes located on the west and east- (left and right-) facing sides of the Allison tornado (their Fig. 6), and not directly in front of the tornado (i.e., on the northern side), W99 note an irregularity or spike in the Allison pressure trace (their Fig. 14), which was assumed to be caused by secondary vortices in or near the main tornado vortex, "at a radius near that of the maximum velocity," as described in the Lewellen et al. (1997) numerical simulation. This likely is akin to the DMH22 Pilger, NE EF4 west in-situ observations of the orbiting vortex, or satellite vortex as defined in Edwards (2014). Due to the placement of the W99 probes on the lateral sides of the Allison tornado, W99 did not sample the area immediately northeast of (i.e., upstream), or directly in front of, the tornado, where O17 and O18 propose the VVS and PDL regions to be. The frontal sampling also was where the PACRITEX research team recorded the quick dips and rises in pressure during the Tulsa, Burnsville, and McCook tornadoes prior to each impacting the INPAR probe, analogous to the Blair et al. (2008) and a number of the K10 observations.

WS04 specifically highlights two individual pressure-deficit spikes lasting ≤10 s during and after the Stratford tornado's core passage (Fig 15; shown as Vortex a & b). The spikes were thought to be associated with sub-tornado-scale vortices, comparable to W99, K10, and likely the Tulsa in-situ observations and

findings. Of more importance for this study is the length of time the Samaras HITPR experienced these pressure fluctuations prior to the Stratford core-flow passage. Figure 15 shows the first pressure depression by 127 s, followed by dips and rises through 162 s, with a final rise near 178 s, before the deficit accompanying the Stratford main tornado core. The HITPR experienced pressure fluctuations for ≈53 s before the main Stratford tornado core passage, similar to the McCook pressure trace.

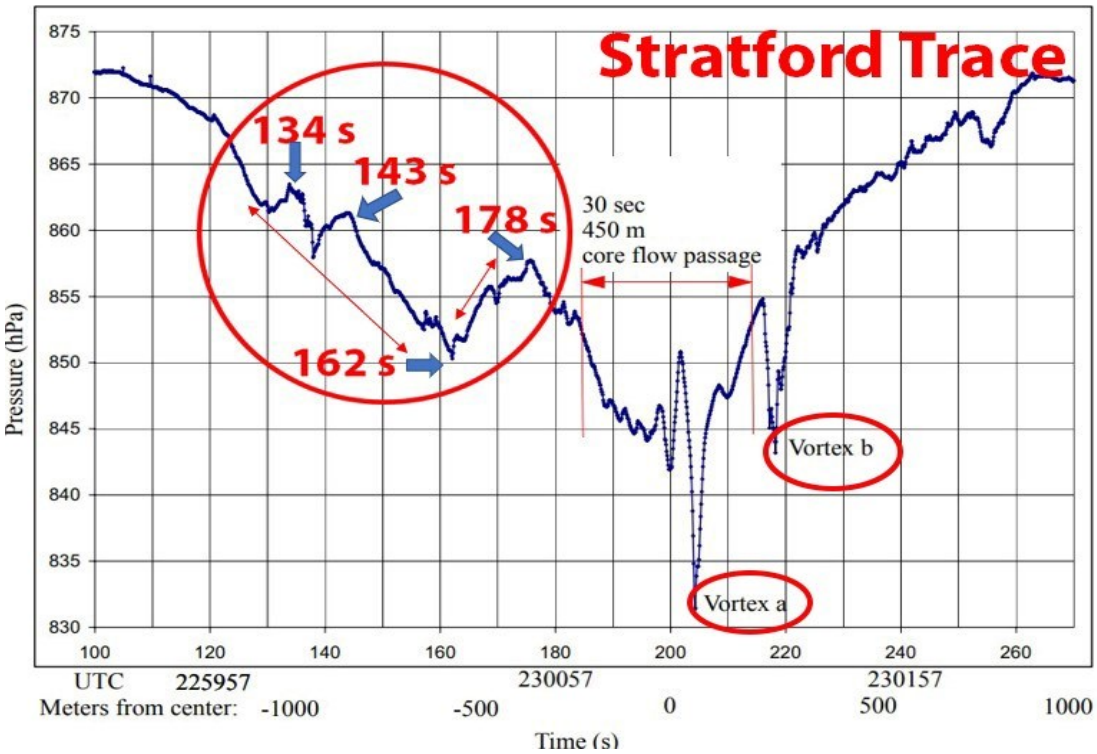

Figure 15: 15 May 2003 Stratford, TX pressure trace showing time in seconds of pressure fluctuations before the main tornado pressure deficit. Pressure fluctuations are circled in red. Time in seconds highlighted in red. Adapted from Fig. 3 in Wurman and Samaras (2004).

While most of the pressure deficits over the WS04 53 s timespan could be attributed to a large, near-surface LLM, there are some inconsistencies in timing and deployment location with respect to the first few pressure fluctuations. K10 suggested the WS04 pre-tornado pressure fluctuations captured cascading of vortices from the LLM to the tornado core. However, WS04 describes the HITPR being deployed upstream of the 400–m-wide Stratford tornado in what appears to be part of the FFDD core, near where it attaches to the hook echo. That position possibly resembles S13 and G18, with a small area of lower reflectivity to the immediate northeast of the tornado core (Figs. 5, 6 in WS04). This suggests that the WS04 pressure fall starting near 123 s, followed by sharp pressure fluctuations (i.e., dips and spikes) from near 127 s through near 143 s (Fig. 15), were recorded in a portion of the downdraft, immediately adjacent to and upstream of the LLM/tornado core. As such, they could not be associated with the LLM surface pressure falls. Therefore, these small deficits may be related to the possible O18 PDL or S13 and G18 LRR vortices, and by proxy, the VVS. Presumably, the pressure fluctuations seen before the Stratford tornado core passage over the HITPR are not irregularities at all, but likely are a manifestation of the sampling-rate ability. During the WS04 in-situ observations, the Samaras HITPR sampled at 10 Hz with future plans to increase the sampling rate (Samaras 2007, personal communication).

In comparison, the Blair et al. (2008) and K10 MM observations sampled at 1 Hz. While a pressure-deficit fluctuation is clearly seen in the Blair et al. (2008) trace, prior to the main Tulia tornado deficit and many of the K10 MM

observations, those traces are less defined. Simply stated, the WS04 HITPR sampling rate of 10 Hz allowed for finer resolution compared to the Blair et al. (2008), K10 MM, and Burnsville, MS sampling rates of 1 Hz. Due to the WS04 HITPR deployment location in relation to the Stratford FFDB, LLM, and tornado core, the 10-Hz sampling rate could have assisted in capturing some portion of the proposed O18 VVS or PDL, as highlighted in Fig. 1, during the WS04 53-s pressure fluctuations.

Although the INPAR sampling rate during the Tulsa event was coded at 20 Hz (40 Hz in forced mode) for testing purposes, the sampling rate during the Burnsville tornado was re-coded at 1 Hz. This likely is why the Burnsville pressure trace looks similar to the Blair et al. (2008) trace. To increase the overall sampling resolution, the lead author increased the INPAR sampling rate to 40 Hz (forced mode) roughly one month before the McCook deployment. This provided increased resolution, as seen in Fig. 14, compared to the Burnsville trace (Fig.12a). The authors are unaware of any formal in-situ pressure-deficit observations with a sampling rate >10 Hz, making the Tulsa and McCook data unique, and likely the highest successful near and in-situ sampling rates during any field project to date.

While the Tulsa, McCook, and WS04 pressure traces share some similarities, particularly during the 65-s deficit prior to the McCook tornado sideswiping the INPAR, in-depth video analysis shows no visible secondary vortices present at any time. This suggests that the 65-s hovering pressure was not caused by secondary or even possible VVS vortices. Moreover, since the McCook tornado did not impact the probe directly, and because no outstanding features were observed like in the Burnsville event (i.e., bowl lowering), one has to question what caused the McCook 65-s deficit before the McCook tornado affected the INPAR.

Arguably, the McCook 65-s deficit captures the LLM surface pressure. However, because the INPAR deployment location was upstream of the McCook tornado, near the FFCB and proposed O18 VVS, this location would be near or just inside of the FFDD with downdraft properties, and may not be associated with the immediate LLM updraft. Another argument could be made that the 65-s deficit is a possible capture of at least some portion of the proposed O18 SVC PDL, occurring some distance ahead of the McCook LLM/tornado (possibly similar to WS04). The location of the INPAR in relation to the McCook FFDB, possible VVS, vortex location, and direction of travel correlate well with the INPAR possibly sampling some portion of the O17, O18, and O20 PDL, as highlighted in Fig. 1. However, because the pressure traces would likely look similar regardless, it is inconclusive what this feature actually is.

7. Theoretical concerns and observational considerations

Although both the Tulsa and McCook deployments were successful open in-situ deployments (i.e., not partial deployments like Burnsville), the erratic nature of the Burnsville tornado and chaotic deployment limited the research team from removing the probe completely out of the vehicle prior to the Burnsville tornado impact. Thus, the INPAR remained partially inside the vehicle at a height of roughly 0.61 m (2 ft). While probe video shows two of the four pressure ports facing into the wind, the two remaining pressure ports were facing directly into the rear of the vehicle. With only two wind-facing ports, the flow field may have been highly disrupted compared to open in-situ deployments (e.g., Lee et al. 2004; Samaras 2006). The associated effects on the Burnsville recorded pressure trace are unclear. The flow-field dynamics around the portion of the probe that was partially inside the vehicle are beyond the scope of this study, as are the flow effects around and through the vehicle at the time of deployment. The authors recognize and concede that the disrupted flow field is an issue of possible contention among reviewers and readers alike. Regardless, even with limited wind-facing pressure ports, the 41-hPa pressure deficit is quite respectable, given the questionable flow field with regards to the angular dependence.

While the wind-tunnel data reflect a high degree of accuracy of the INPAR probe and pressure sensor (discussed in Section 3), due to the INPAR probe's remaining partially inside the research vehicle during the Burnsville partial in-situ deployment, concern remains with exact calculations of angular dependence. While the wind-tunnel tests attempted to replicate this scenario (Fig. 5b and Fig. 6), with some limited success, the authors are not confident with the estimated wind velocity findings below 40 m s^{-1} due to the X/L and C_p dependence (Fig. 5) and the disrupted flow field. Nevertheless, INPAR

probe data during the Burnsville impact reveal just over 54 m s^{-1} peak estimated windspeed (Fig. 12b) as the tornado core passed roughly 1–3 m (6–12 ft) from the INPAR and research team and the documentation of the 41-hPa pressure deficit (Fig. 12a) correlates well with previous near and in-situ observations in similar scenarios (e.g., K10; Lee at al. 2004; Lee et al. 2011; WS04).

8. Summary and discussion

From the spring of 2016 through the spring of 2019, three EF2-rated tornadoes were sampled with INPAR tornado probes near and in situ. Probe pressure measurements obtained during the 30 March 2016 Tulsa, OK, EF2 tornado were characterized by multiple pressure fluctuations prior to the tornado impacting the INPAR probe. Initial pressure measurements during the Tulsa event were recorded near the FFDB and FFCB, just ahead of the approaching main tornado core. In the Tulsa case, a second absolute pressure-deficit maximum of 45 hPa below ambient occurred roughly 8 s after the main tornado impacted the probe. This second pressure deficit maxima is likely associated with a secondary vortex, and will be discussed in a future publication. Due to the Tulsa pressure findings, and through multiple collaborations and study of the large-eddy simulation research work of O17/O18, the PACRITEX field research campaign set out to further sample/study meteorological variables near and within the FFDB and FFCB, and in-situ to tornadoes, to document pressure deficits thought to be associated with the possible SVC, or more precisely, within the related O18 VVS and PDL regions during the 2019 severe-weather season.

During the PACRITEX 2019 field campaign, two EF2-rated tornadoes were intercepted, one near Burnsville, MS, with a partial deployment of an INPAR probe, and the other successful deployment of an INPAR probe near McCook, NE, recording pressure, temperature, humidity, and calculated wind velocities. Results from those events revealed pressure-deficit fluctuations of roughly 4–13 hPa documented upstream (i.e., in front) of each respective tornado prior to larger pressure deficits associated with each tornado vortex, similar to the 30 March 2016 Tulsa, OK EF2 event.

In the Burnsville, MS case, video observations highlight a unique rotating bowl feature that passed near or directly over the PACRITEX research team. Strict pressure-trace investigation shows a roughly 5-hPa deficit believed to be associated with the passage of the bowl feature, before the large 41-hPa pressure deficit associated with the Burnsville tornado core. The bowl feature correlates in location with the O17, O18, O20, and F23 simulations of a possible VVS vortex, independent of the Burnsville tornado and immediate inflow layer, that was moving toward the Burnsville tornado. Review of the Wurman et al. (2012), S13, and Kosiba et al. (2013) observations may support the bowl feature possibly being associated with a LRR, while G18 may support the bowl feature being associated with an LRR formation stage near or within the FFDB.

During the McCook, NE case, a pressure deficit of ≈6 hPa was documented, lasting ≈65 s before the pressure rose and then abruptly fell as the outer winds of the tornado core obliquely sideswiped the INPAR probe. The authors have shown that the McCook 6-hPa hovering pressure deficit correlates in location with the O17 and O18 possible PDL location, ahead and immediately north of the tornado vortex (Fig. 1), but near the FFDB and possible VVS. Still, the LLM plausibly could be responsible for the 6-hPa deficit, as part of cascading pressure described by K10. Although the McCook 65 s pressure data partially may support the K10 cascade of vortices in theory, particularly the capture of the LLM pressure, visual and first-person observations do not definitively support this scenario. Video observations appear to show the LLM and tornado core some distance to the southwest of INPAR during the 65-s deficit. Due to the deployment location of the INPAR in relation to the FFDB, possible VVS, and McCook LLM, the 65-s, 6-hPa pressure deficit could be a capture of at least some portion of the possible O17, O18, O20, F18, and F23 PDL (Fig. 1).

While the WS04, K10, and Blair et al. (2008) near and in-situ observations may have documented the possible O17 and O18 VVS and PDL, and likely the S13 and G18 LRR vortices, as seen in their respective pressure traces, the authors believe that the documentation of the Burnsville and McCook pressure fluctuations, along with the visual observations of the Burnsville bowl feature, could be the first-recognized observations of the possible O18 VVS and PDL. However, additional in-situ observations within the possible VVS and PDL regions will be necessary to determine

whether pressure deficits, like those recorded during the Tulsa, Burnsville, and McCook events, can be replicated and distinguished between the LLM surface pressure falls. The authors hope that this study's pressure and visual documentation will provide continued motivation for additional work and research of the possible O18 VVS and PDL regions.

As described in section 4, the INPAR was validated in a wind tunnel with wind velocities up to 55 m s^{-1}. Results of the wind-tunnel test confirmed the INPAR capable of measuring static pressure in high-wind environments such as tornado cores, with a high degree of accuracy, and show the INPAR is comparable to the SL04 HITPR. Previous INPAR in-situ video observations during the Pilger, NE EF4 west tornado (DMH22) highlight the robust nature and survivability of the INPAR in-situ tornado probe. Thus, the INPAR is well suited to accurately measure the static pressure near and in tornado cores and supercells, particularly with windspeeds near and above 40 m s^{-1}.

ACKNOWLEDGMENTS

The authors wish to dedicate this paper to the late Paden Nichols Joy-Gordon. Paden was an integral part of the PACRITEX research team with a passion for all things weather-related. Paden was instrumental in the research for this study, but more importantly, he was a dear friend and will be sorely missed. The authors wish to thank Roger Edwards for his patience. From replying to late-night emails and messages to answering elementary questions, Roger embodies what a scientist should be and makes those around him want to do and be better. Sincere gratitude to Dr. Leigh Orf for collaboration and sharing his vast knowledge. Many thanks to Mike Johnson and the entire NWS Memphis staff for collaborating. The authors wish to personally thank Jon Davies and Austin Bray for sharing suggestions on this manuscript and giving support. The authors also thank James Aydelott, James Shelby, Josh Napper, Rich Thompson, and Cameron Nixon. And finally, the authors thank reviewers Jana Houser, Kelton Halbert, and Sean Waugh for their comments and suggestions in contributing to the improvement of this manuscript. Special gratitude to Sean Waugh who gave valuable personal time and words of encouragement through this process.

APPENDIX

Burnsville Video Links:

Burnsville deployment location 1 video

Burnsville reposition video

Burnsville inflow video 1

Burnsville bowl lowering video

Burnsville corner flow video

Burnsville impact 1 video

McCook Video Links:

McCook tornado video 2 FULL

Contact Lanny Dean for data availability at led42@msstate.edu

REFERENCES

Adlerman, E. J., and K. K. Droegemeier, 2002: The sensitivity of numerically simulated cyclic mesocyclogenesis to variations in model physical and computational parameters. *Mon. Wea. Rev.*, **130**, 2671–2691.

——, and ——, 2005: The dependence of numerically simulated cyclic mesocyclogenesis upon environmental vertical wind shear. *Mon. Wea. Rev.*, **133**, 3595–3623.

——, ——, and R. Davies-Jones, 1999: A Numerical Simulation of Cyclic Mesocyclogenesis. *J. Atmos. Sci.*, **56**, 2045–2069.

Arnold, R. T., H. E. Bass, and L. N. Bolen, 1976: Acoustic spectral analysis of three tornadoes. *J. Acoust. Soc. Amer.*, **60**, 548–593, doi: https://doi.org/10.1121/1.381132.

Beck, J., and C. C. Weiss, 2013: An assessment of low-level baroclinity and vorticity within a simulated supercell. *Mon. Wea. Rev.*, **141**, 649–669.

——, J. L. Schroeder, and J. M. Wurman, 2006: High-resolution dual-Doppler analyses of the 29 May 2001 Kress, Texas, cyclic supercell. *Mon. Wea. Rev.*, **134**, 3125–3148

Bedard, A. J., and C. Ramzy, 1983: Surface meteorological observations in severe thunderstorms. Part 1: Design details of TOTO. *J. Appl. Meteor.,* **22**, 911–918.

——, and T. M. Georges, 2000: Atmospheric infrasound. *Phys. Today*, **53**, 32–37.

——, 2005: Low-frequency atmospheric acoustic energy associated with vortices produced by thunderstorms. *Mon. Wea. Rev.*, **133**, 241–263.

Blair, S. F., D. R. Deroche, and A. E. Pietrycha., 2008: In situ observations of the 21 April 2007 Tulia, Texas tornado. *Electronic J. Severe Storms Meteor.*, **3** (3), 1–27.

Bluestein, H. B., 1983: Surface meteorological observations in severe thunderstorms. Part II: Field experiments with TOTO. *J. Appl. Meteor. Climatol.*, **22**, 919–930.

——, 1999: A history of severe-storm-intercept field programs. *Wea. Forecasting*, **14**, 558–577.

——, W. Lee, M. Bell, C. C. Weiss, and A. L. Pazmany, 2003: Mobile Doppler radar observations of a tornado in a supercell near Bassett, Nebraska, on 5 June 1999. Part II: Tornado-vortex structure. *Mon. Wea. Rev.*, **131**, 2968–2984.

——, Houser, J. B., M. M. French, J. C. Snyder, G. D. Emmitt, I. PopStefanija, C. Baldi, and R. T. Bluth, 2014: Observations of the boundary layer near tornadoes and in supercells using a mobile, collocated, pulsed Doppler lidar and radar. *J. Atmos. Oceanic Tech.*, **31**, 302–325.

Boustead, M. J., and P. N. Schumacher 2008: The development of multiple low-level mesocyclones within a supercell. Proc., *24th Conf. on Severe Local Storms*, Madison, WI, Amer. Meteor. Soc., P3.17.

Brock, F. V. (1987): Measurements of pressure and air temperature near severe thunderstorms: An inexpensive and portable instrument. Preprints, *Sixth Symp. on Meteorological Observations and Instrumentation*, New Orleans, LA, Amer. Meteor. Soc., 320–323.

——, K. C. Crawford, R. L. Elliott, G. W. Cuperus, S. J. Stadler, H. L. Johnson, and M. D. Eilts, 1995: The Oklahoma Mesonet: A technical overview. *J. Atmos. Oceanic Technol.*, **12**, 5–19.

Brooks, E. M., 1949: The tornado cyclone. Weatherwise, **2**, 32–33.

Broyles, J. C., C. K. Potvin, J. Murnan, S. Shores, A. D. Lyons, M. S. Elliott, and A. R. Cook, 2022: Tornadogenesis in high-end tornadic supercells, Part 2: The descending reflectivity core, inflow channel and streamwise vorticity current. Proc., *30th Conf. on Severe Local Storms*, Santa Fe, NM, Amer. Meteor. Soc., P13.

Browning, K. A., and C. R. Landry, 1963: Airflow within a tornadic storm. Preprints, *10th Weather Radar Conf.*, Washington, DC, Amer. Meteor. Soc., 1116–1112.

Burgess, D. W., V. T. Wood, and R. A. Brown, 1982: Mesocyclone evolution statistics. Preprints, *12th Conf. on Severe Local Storms*, San Antonio, TX, Amer. Meteor. Soc., 422–424.

Coffer, B. E., M. D. Parker, J. M. Peters, and A. R. Wade, 2023: Supercell low-level mesocyclones: Origins of inflow and vorticity. *Mon. Wea. Rev.*, **151**, 2205–2232.

Dahl, J. M. L., 2017: Tilting of horizontal shear vorticity and the development of updraft rotation in supercell thunderstorms. *J. Atmos. Sci.*, **74**, 2997–3020.

——, M. D. Parker, and L. J. Wicker, 2014: Imported and storm-generated near-ground vertical vorticity in a simulated supercell. *J. Atmos. Sci.*, **71**, 3027–3051.

Davies, J. M., C. A. Doswell III, D. W. Burgess, and J. F. Weaver, J. F., 1994: Some noteworthy aspects of the Hesston, Kansas, tornado family of 13 March 1990. *Bull. Amer. Meteor. Soc.*, **75**, 1007–1018.

Davies-Jones, R. P., 1984: Streamwise vorticity: The origin of updraft rotation in supercell storms. *J. Atmos. Sci*, **41**, 2991–3006.

——, and H. E. Brooks, 1993: Mesocyclogenesis from a theoretical perspective. The Tornado: Its Structure, Dynamics, Predication, and Hazards. *Geophys. Monogr.*, Vol. 79, Amer. Geophys. Union, 105–114.

——, Trapp. R. J., and H. B. Bluestein, 2001: Tornadoes and tornadic storms. *Severe Convective Storms, Meteor. Monogr.,* No. 50, Amer. Meteor. Soc., 167–221.

Dean, L. E., D. R. Moran, and R. D. Hicks, 2022: In-situ video observations and analysis of the 16 June 2014 Pilger, Nebraska EF4 west tornado. *Electronic J. Severe Storms Meteor.*, **17** (3), 1–28.

Dowell, D. C., and H. B. Bluestein, 1997: The Arcadia, Oklahoma, storm of 17 May 1981: Analysis of a supercell during tornadogenesis. *Mon. Wea. Rev.*, **125**, 2562–2582.

——, and ——, 2002: The 8 June 1995 McLean, Texas, storm. Part I: Observations of cyclic tornadogenesis. *Mon. Wea. Rev.*, **130**, 2626–2648.

Edwards, R., and A. R., Dean, 2018: Environments of supercellular satellite tornadoes. Proc., *29th Conf. on Severe Local Storms*, Stowe, VT, Amer. Meteor. Soc., 51.

——, 2014: Characteristics of supercellular satellite tornadoes. Proc., *27th Conf. on Severe Local Storms*, Madison, WI, Amer. Meteor. Soc., 17.5.

Finley, C. A., L. Orf, B. D. Lee, and R. B. Wilhelmson, 2018: High-resolution simulation of a violent tornado in the 27 April 2012 outbreak environment. *29th Conf. on Severe Local Storms*, Stowe, VT, *Amer. Meteor. Soc*., 10B.5.

——, Elmore, M., Orf, L., & Lee, B., D 2023: Impact of the streamwise vorticity current on the low-level mesocyclone development in a simulated supercell. *Geophys. Res. Lett.,* **50***,* e2022GL100005.

French, M. M., H. B. Bluestein, D. C. Dowell, L. J. Wicker, M. R. Kramar, and A. L. Pazmany, 2008: High-resolution, mobile Doppler radar observations of cyclic mesocyclogenesis in a supercell. *Mon. Wea. Rev.*, **136**, 4997–5016.

Fujita, T., 1958: Mesoanalysis of the Illinois tornadoes of 9 April 1953. *J. Atmos. Sci.*, **15**, 288–296.

Georges, T. M., and G. E. Greene, 1975: Infrasound from convective storms. Part IV. Is it useful for storm warning?. *J. Appl. Meteor. Climatol.*, **14**, 1303–1316.

Griffin, C. B., C. C. Weiss, A. E. Reinhart, J. C. Snyder, H. B. Bluestein, J. Wurman, and K. A. Kosiba, 2018: In situ and radar observations of the low reflectivity ribbon in supercells during VORTEX2. *Mon. Wea. Rev.*, **146**, 307–327.

Houser, J. L., H. B. Bluestein, and J. C. Snyder, 2015: Rapid-scan, polarimetric, Doppler radar observations of tornadogenesis and tornado dissipation in a tornadic supercell: The "El Reno, Oklahoma" storm of 24 May 2011. *Mon. Wea. Rev.*, **143**, 2685–2710.

Karstens, C. D., T. M. Samaras, B. D. Lee, W. A. Gallus Jr., and C. A. Finley, 2010: Near-ground pressure and wind measurements in tornadoes. *Mon. Wea. Rev.*, **138**, 2570–2588.

Klemp, J. B., and R. Rotunno, 1983: A study of the tornadic region within a supercell thunderstorm. *J. Atmos. Sci.*, **40**, 359–377.

Kosiba, K, and J. Wurman, J. 2013: The three-dimensional structure and evolution of a tornado boundary layer. *Wea. Forecasting*, **28**, 1552–1561.

——, J. Wurman, Y. Richardson, P. Markowski, P. Robinson, and J. Marquis, 2013: Genesis of the Goshen County, Wyoming, tornado on 5 June 2009 during VORTEX2. *Mon. Wea. Rev.*, **141**, 1157–1181.

Kumjian, M. R., A. V. Ryzhkov, V. M. Melnikov, and T. J. Schuur, 2010: Rapid-scan super-resolution observations of a cyclic supercell with a dual-polarization WSR-88D. *Mon. Wea. Rev.*, **138**, 3762–3786.

Lee, B. D., T. M. Samaras, and C. R. Young, 2004: Pressure measurements at the ground in an F-4 tornado. Preprints, *22nd Conf. on Severe Local Storms,* Hyannis, MA, Amer. Meteor. Soc., 15.3.

——, Finley, C. A., and Samaras, T. M., 2011: Surface analysis near and within the Tipton, Kansas, Tornado on 29 May 2008. *Mon. Wea. Rev.,* **139**, 370–386.

Lemon, L. R., and C. A. Doswell, 1979: severe thunderstorm evolution and mesocyclone structure as related to tornadogenesis. *Mon. Wea. Rev.*, **107**, 1184–1197.

Lewellen, W. S., 1976: Theoretical models of the tornado vortex. Preprints, *Symp. on Tornadoes; Assessment of Knowledge and Implications for Man,* Texas Tech. University, Lubbock, TX, 107–143.

——, D. C. Lewellen, and R. I. Sykes, 1997: Large-eddy simulation of a tornado's interaction with the surface. *J. Atmos. Sci*, **54**, 581–605.

Lewellen, D. C., and W. S. Lewellen, 2007: Near-surface intensification of tornado vortices. *J. Atmos. Sci.*, **64**, 2176–2194.

Lewis, W., and P. J. Perkins, 1953: Recorded pressure distribution in the outer portion of a tornado vortex. *Mon. Wea. Rev.,* **81**, 379–385.

Lilly, D. K., 1982: Generation and concentration of vertical vorticity. *Intense Atmospheric Vortices*, Springer, 151–160.

Markowski, P. M., and Coauthors, 2012: The pretornadic phase of the Goshen County, Wyoming, supercell of 5 June 2009 intercepted by VORTEX2. Part I: Evolution of kinematic and surface thermodynamic fields. *Mon. Wea. Rev.*, **140**, 2887–2915.

——, Y. P. Richardson, and G. H. Bryan, 2014: The origins of vortex sheets in a simulated supercell thunderstorm. *Mon. Wea. Rev.*, **142**, 3944–3954.

——, T. P. Hatlee, and Y. P. Richardson, 2018: Tornadogenesis in the 12 May 2010 supercell thunderstorm intercepted by VORTEX2 near Clinton, Oklahoma. *Mon. Wea. Rev.*, **146**, 3623–3650.

McPherson, R. A., and Coauthors, 2007: Statewide monitoring of the mesoscale environment: A technical update on the Oklahoma Mesonet. *J. Atmos. Oceanic Technol.*, **24**, 301–321.

Murdzek, S. S., P. M. Markowski, and Y. P. Richardson, 2020: Simultaneous dual-Doppler and mobile mesonet observations of streamwise vorticity currents in three supercells. *Mon. Wea. Rev.*, **148**, 4859–4874.

National Research Council 2009: *Observing Weather and Climate from the Ground up: A Nationwide Network of Networks.* National Academies Press, 234 pp. [Available online at https://nap.nationalacademies.org/read/12540/chapter/1.]

NWS 2016: Tornado events in eastern Oklahoma and northwest Arkansas. [Available online at https://www.arcgis.com/apps/MapJournal/index.html.]

Orf, L., 2020: A 10-m resolution quarter-trillion gridpoint tornadic supercell simulation. Proc., *Severe Local Storms Symp.*, Boston, MA, Amer. Meteor. Soc., 2.1.

——, R. Wilhelmson, B. Lee, C. Finley, and A. Houston, 2017: Evolution of a long-track violent tornado within a simulated supercell. *Bull. Amer. Meteor. Soc*., **98**, 45–68.

——, A. Dixon, and K. T. Halbert, 2018: The role of the streamwise vorticity current in tornado genesis and maintenance. Proc., *29th Conf. on Severe Local Storms*, Stowe, VT, Amer. Meteor. Soc., 1.4.

Rasmussen, E. N., J. M. Straka, M. S. Gilmore, and R. P. Davies-Jones, 2006: A preliminary survey of rear-flank descending reflectivity cores in supercell storms. *Wea. Forecasting*, **21**, 923–938.

Rotunno, R., 1977: Numerical simulation of a laboratory vortex. *J. Atmos. Sci.*, **34**, 1942–1956.

——, 1979: A study in tornado-like vortex dynamics. *J. Atmos. Sci.*, **36**, 140–155.

——, 1981: On the evolution of thunderstorm rotation. *Mon. Wea. Rev.*, **109**, 577–586.

——, 1984: An investigation of a three-dimensional asymmetric vortex. *J. Atmos. Sci*, **41**, 283–298.

——, and J. B. Klemp, 1982: The influence of the shear-induced pressure gradient on thunderstorm motion. *Mon. Wea. Rev.*, **110**, 136–151.

——, and ——, 1985: On the rotation and propagation of simulated supercell thunderstorms. *J. Atmos. Sci.*, **42**, 271–292.

Samaras, T. M., 2006: Dynamic measurements of the lowest 10 meters of tornadoes. Preprints, *23rd Conf. on Severe Local Storms*, St. Louis, MO, Amer. Meteor. Soc., 14.3.

——, and J. J. Lee, 2004: Pressure measurements within a large tornado. Preprints, *Eighth Symp. on Integrated Observing and Assimilation Systems for Atmosphere, Oceans, and Land Surface* Seattle, WA, Amer. Meteor. Soc., 4.9, 1–9.

Satrio, M., 2023: A kinematic and thermodynamic analysis of the 17 May 2019 McCook/Farnam, Nebraska tornadic supercell. Ph.D. dissertation, University of Oklahoma. https://shareok.org/handle/11244/338761.

Schenkman, A. D., M. Xue, and M. Hu, 2014: Tornadogenesis in a high-resolution simulation of the 8 May 2003 Oklahoma City supercell. *J. Atmos. Sci*., **71**, 130–154.

Schueth, A., C. C. Weiss, and J. M. L. Dahl, 2021: Comparing observations and simulations of the streamwise vorticity current and the forward-flank convergence boundary in a supercell storm. *Mon. Wea. Rev*., **149**, 1651–1671.

Skinner, P. S., C. C. Weiss, M. M. French, H. B. Bluestein, P. M. Markowski, and Y. P. Richardson, 2014: VORTEX2 observations of a low-level mesocyclone with multiple internal rear-flank downdraft momentum surges in the 18 May 2010 Dumas, Texas, supercell. *Mon. Wea. Rev.*, **142**, 2935–2960.

Snyder, J. C., H. B. Bluestein, V. Venkatesh, and S. J. Frasier, 2013: Observations of polarimetric signatures in supercells by an X-band mobile Doppler radar. *Mon. Wea. Rev.*, **141**, 3–29.

Stout, G. E., and F. A. Huff, 1953: Radar records Illinois tornadogenesis. *Bull. Amer. Meteor. Soc.*, **34,** 281–284.

Tatom, F. B., K. R. Knupp, and S. J. Vitton, 1995: Tornado detection based on seismic signal. *J. Appl. Meteor. Climatol.*, **34**, 572–582.

Tepper, M., and W. E. Eggert, 1956: Tornado proximity traces. *Bull. Amer. Meteor. Soc.*, **37**, 152–159.

Van Tassel, E. L., 1955: The North Platte Valley tornado outbreak of June 27, 1955. *Mon. Wea. Rev.*, **83**, 255–264.

Wakimoto, R. M., C. Liu, and H. Cai, 1998: The Garden City, Kansas, storm during VORTEX 95. Part I: Overview of the storm's life cycle and mesocyclogenesis. *Mon. Wea. Rev.*, **126**, 372–392.

Ward, N. B., 1972: The exploration of certain features of tornado dynamics using a laboratory model. *J. Atmos. Sci*., **29**, 1194–1204.

Weiss, C. C., and J. L. Schroeder, 2008: StickNet—A new portable, rapidly deployable, surface observation system. Preprints, *24th Conf. on IIPS*, New Orleans, LA, Amer. Meteor. Soc., P4A.1.

Wicker, L. J., and R. B. Wilhelmson, 1995: simulation and analysis of tornado development and decay within a three-dimensional supercell thunderstorm. *J. Atmos. Sci.*, **52**, 2675–2703.

Wilhelmson, R. B., and J. B. Klemp, 1978: A numerical study of storm splitting that leads to long-lived storms. *J. Atmos. Sci.*, **35**, 1974–1986.

Wienhoff, Z. B., H. B. Bluestein, D. W. Reif, R. M. Wakimoto, L. J. Wicker, and J. M. Kurdzo, 2020: Analysis of debris signature characteristics and evolution in the 24 May 2016 Dodge City, Kansas, tornadoes. *Mon. Wea. Rev.*, **148**, 5063–5086.

Winn, W. P., Hunyady, S. J., and Aulich, G., 1999: Pressure at the ground in a large tornado. *J. Geophys. Res.,* **104**, 22067–22082.

Wurman, J., and K. Kosiba, 2013: Finescale radar observations of tornado and mesocyclone structures. *Wea. Forecasting*, **28**, 1157–1174.

——, and T. Samaras, 2004: Comparison of in-situ pressure and DOW Doppler winds in a tornado and RHI vertical slices through 4 tornadoes during 1996–2004. Preprints, *22nd Conf. on Severe Local Storms,* Hyannis, MA, Amer. Meteor. Soc., 15.4, 1–14.

——, D. Dowell, Y. P. Richardson, P. M. Markowski, E. N. Rasmussen, D. W. Burgess, L. J. Wicker, and H. B. Bluestein, 2012: The second Verification of the Origins of Rotation in Tornadoes Experiment: VORTEX2. *Bull. Amer. Meteor. Soc.*, **93**, 1147–1170.

Wurman, J. 2008: Deployments of a 12-site in situ wind/T/RH instrument array in tornadoes. Proc., *24th Conf. on Severe Local Storms*, Madison, WI, Amer. Meteor. Soc., 8B.4.

——, ——, P. Robinson, and T. P. Marshall, 2014: The role of multiple-vortex tornado structure in causing storm researcher fatalities. *Bull. Amer. Meteor. Soc.*, **95**, 31–45.

Xia, J., W. S. Lewellen, and D. C. Lewellen, 2003: Influence of Mach number on tornado corner flow dynamics. *J. Atmos. Sci.*, **60**, 2820–2825.

REVIEWER COMMENTS

[Authors' responses in *blue italics.*]

REVIEWER A (Sean M. Waugh):

Initial Review:

Recommendation: Accept with major revisions.

Overall Comments: The manuscript is well written and provides unique observations of exceptionally hard to observe environments, observations that are well worth publishing. There are a few formatting issues and some minor comments that I have noted, as well as a few major comments that I would like to see addressed, but I believe that the manuscript is very close to ready for publication and have the utmost confidence that the authors can handle the suggested modifications. I commend the authors for a job well done, both on the manuscript and the data collection efforts, which are by no means an easy feat.

Thank you so much for your helpful and insightful review, which we believe has led to much improvement in our manuscript. We believe we have addressed all or most issues/comments. Specific responses to each comment are included below (major comments first…). Due to Sean's expertise in sensors, design, implementation, and deployment, his review is much appreciated! Please note: Because major revisions were made in response to all reviewers, this study has undergone a major overhaul with many changes including but not limited to: section rearrangements/additions, figure addition/retractions, reference/citing additions, overall language/overtone adjustments, and many other minor/major changes. Of particular importance, I've added our Tulsa, OK, in-situ observations to this study, thus the title change of the paper to: "Pressure Measurements and Video Observations Near and Inside Three EF2 Tornadoes." We believe the addition of the Tulsa event strongly helps to further lay foundation for reviewers and readers alike.

Major Comments: There are four pressure ports on the exterior of the probe at 90° increments around a circle. The authors state that the wind direction can be determined by examining the pressure values from these ports as the pressure will be higher on the wind facing side and lower on the lee side of the probe. However, the text would imply that the highest pressure port observation is set as the wind direction, which would force the wind direction to be one of four options given the four pressure ports as you have no information between the ports. Can the authors comment on the resolution ability of the probe and whether it can resolve wind directions on scales smaller than 45° increments? Is there an interpolation done to derive the wind direction on a finer scale?

While this is mostly correct, I think it is important to note that we state: "estimated wind direction" and, "the pressure port measuring the highest/lowest pressure is the port the wind is coming from (e.g., the direction the wind is blowing)". Due to the placement of four pressure ports with a radius of 13 cm, the angular variation could be measured simultaneously. Since the pressure is highest in the direction facing the wind (new Fig. 5b), the pressure port with the highest/lowest pressure will indicate the direction from which the wind is coming. The measurement at this point is equal to the free-stream static pressure. Once the direction of the wind is known, the static free-stream pressure is also known. This can be validated in SL04 and the adapted Eq. 4. However, we believe we recognize the reviewer's point, and I have slightly amended verbiage here. Additionally, the validation of this can be seen in the new Fig. 5b (wind-tunnel windspeed vs. INPAR calculated/estimated windspeed) showing the actual "real" windspeed vs. the probe calculated windspeed (as also requested by the reviewer below). As one can see, the accuracy increased as the estimated/calculated wind speed increased as C_p became independent of X/L from near 40–43 through 55 m s^{-1}. Due to reviewer #2 questions, I've shown this with exact values through each respective Q (applied wind speed within the wind tunnel). I believe I have now clearly explained and shown the X/L C_p dependence and accuracy questions/concerns.

During the Burnsville tornado, the INPAR was "deployed" in the back of the vehicle due to the conditions of the deployment described in the manuscript. While the INPAR would have been exposed to the ambient environment to a degree, this is not a true exposure as it would be modified by the vehicle. The pressure

certainly dropped as the tornado passed and the timing is correct, but the magnitude of the pressure drop is in question as flow over, around, and through the vehicle at this time could be causing localized pressure effects that would ultimately bias the pressure observations (either high or low depending on the flow). Furthermore, as the probe is sitting in a semi-enclosed space, this would naturally funnel the wind and pressure field through the vehicle, which would modify the natural wind field. While the data can be shown, I think it should be made clear that there are significant concerns with the applicability of the data and resultant wind calculations. Edit—this is somewhat addressed later in section 6, though I think a few additional points can be made as I note in comment 5. I would suggest adding a more forceful statement here. Something like: "Given the issues during deployment into the Burnsville tornado, the data presented here are in question as numerous unintended influences could be biasing the observations. As such, the observations are presented here for documentation and should be considered estimates only and should be used with caution."

Agreed, although it seems important to understand "partially deployed on" not in the back of the vehicle per se. While we believe we have made our concerns with the Burnsville data abundantly clear, I have amended much of this section. Additionally, I've added: "Given the issues during deployment into the Burnsville tornado, the data presented here are in question as numerous unintended influences could be biasing the observations. As such, the observations are presented here for documentation and should be considered estimates only and should be used with caution".

While the information in section 5 showcasing and discussing previous observations from other research is certainly relevant, it feels more like a background discussion that is more appropriate in the introduction to set the stage for the observations presented here. I believe that moving much of this discussion to section 1 in a section titled "Background" would be more appropriate, leaving this section to focus on comparison points from the observations presented here. Furthermore, the numerous observational datasets provided does seem to conflict with an earlier claim in the manuscript regarding an absence of in situ observations. It may be more appropriate to say "extremely limited."

While we recognize and concede the reviewer's point, it was not our intention to showcase section 5 or any part of this study as a background or historical review of in-situ observations, but rather, showcasing the similarities of the roughly 21 previous pressure-deficit observational cases to the Burnsville and McCook (and now Tulsa) and compare all to the O17/O18 and F23 simulations. However, I've added a new sub-section (Background) within the Introduction as suggested. I've given a light background of previous in-situ tornado "probes" citing TOTO (Bedard and Ramzy 1983; Bluestein 1993; 1999) etc. I've also lightly discussed (cited and referenced) a few successful past in-situ documentations describing the "V" shape characteristics of each respective pressure trace and shown the novelty of this study due to comparison of the 21 other in-situ observational case studies to hopefully help give additional background. I have still retained section 5 as previous in situ observational studies, although I've amended much of this section (and most of the paper). Of particular importance is the amended verbiage discussing the possible role of the LLM in the recorded data and the 21 other studies.

While Fig. 14 is certainly relevant, I don't think it tells a complete story for the comparison between the INPAR and the mesonet. Comparing max and min values over entire days leaves out the possibility that these occurred at different times, or were significantly lagged from each other. I strongly suggest that the authors add an additional figure here that shows a 1-to-1 comparison between the INPAR and the mesonet pressure day over the entire 96-h period. I believe the mesonet data is available in either 1-min or 5-min increments, so I would suggest a plot comparing the observations on that scale, matched by time, to allow a direct comparison of the two observations in their entirety. A difference plot could also be created that shows the difference between these observations at each time step.

Agreed. As reviewer #3 suggested, I've combined old section 6 with section 2 and amended much of this section thus, moving old Fig. 14 to new Fig. 4, old Fig. 15 to new Fig. 5a, and the addition of new figure showing the entire 96-hour INPAR vs. OILT test results over time in 5 min. increments, as requested. I've also elaborated on the FS calculations adding two new equations (Eqs. 1 and 2) reflecting total FS calculations, as mentioned by reviewer #3.

The wind-tunnel test and Fig. 15 are slightly confusing to me. It makes sense to put the probe into the wind tunnel, recording the pressure on the INPAR and derive the winds based on that pressure, to compare with what the wind tunnel speed was at a given point. However, I don't get that from the figure as I see raw pressure observations with marked sections of wind speed which I assume are the four wind tunnel speeds tested (22, 33, 43, and 55 m s^{-1}). A figure showing the wind-tunnel speed and the calculated INPAR speed would be informative here to showcase the ability of the INPAR to correctly resolve and derive the appropriate wind speed. Additionally, while the authors mention that this does not represent the exact conditions of the Burnsville tornado, I think additional comments as to the likely influence of the vehicle could be added here to provide context for possible error sources. I mentioned some of this in my second major comment.

Apologies for any confusion regarding old Fig. 15 (new Fig. 4a). However, the reviewer may be misunderstanding wind-tunnel testing. The pressure variations were measured after applying the various wind speeds (as all wind-tunnel tests do to our knowledge)—you cannot record pressure variations without first applying the various wind speeds. If we are understanding the reviewer's question/point, it's just opposite of what the reviewer is saying. The reviewer is correct in that the respective Qs (the Q's are normal verbiage) are indeed the applied/tested windspeed within the wind tunnel and are shown as 22 m s^{-1}, 33 m s^{-1}, 43 m s^{-1} and 55 m s^{-1}. It is believed the reviewer is requesting a basic one to one-to-one windspeed comparison showing the wind speed of the wind tunnel and the calculated speed on/of the INPAR?

Update: After communication with the reviewer and editor, we understand the reviewer is suggesting one to one type comparison of wind tunnel windspeed vs. calculated probe windspeed. As such, I've added a new Fig 4b showing each respective Q (applied windspeed within the wind tunnel during each Q from 22–55 m s^{-1}) and the INPAR calculated windspeed. As seen in Fig.5b, the "dip" or large shift at 22 m s^{-1} through 33 m s^{-1} before becoming more "straight" near 40–43 m s^{-1} through 55 m s^{-1}. This highlights the flow separation at that those lower windspeeds as discussed in Section 3 with the XL and C_p dependence. This "separation" or large shift can also be validated in the Samaras and Lee (2004 literature). Simply stated, the "straightening" of this dip near 40–43+ m s^{-1} (Q3) would indicate C_p being totally independent of XL starting at near 40–43 m s^{-1} continuing through 55 m s^{-1} (Q4) and very accurate, where wind speeds from near 33 m s^{-1} through just below 40 m s^-1 show the calculated wind becomes less accurate, and C_p and XL become slightly dependent. The 22 m s^{-1} (Q1) shows a large dip indicating not accurate, with C_p and XL totally dependent. Hence, the concerns with the estimated wind data accuracy below 40 m s^{-1} as described in this study. Also, we believe Fig. 4b and amended verbiage will assist reviewer #1 and reviewer #2, as well as the readers, in actually "seeing" the X/L C_p dependence ("in action").

[Minor comments omitted…]

Second Review:

Recommendation: Accept with minor revisions.

Overall Comments: Generally, I am happy with the revisions of the manuscript and commend the authors for their work in addressing the concerns of the reviewers. I have a few comments in this document, and have made several suggested modifications in a tracked changes version of the submitted document. I only have one major comment for the authors which I believe is easily addressable. I will mention however, that for some odd reason many figures in the main document appear to be incomplete, with only part of the picture loaded. This very well could be a "me" issue or something wonky with Microsoft Word, but I mention it here so that the authors and editor can be sure to check the final proof to make sure that such issues aren't present there. For example Fig. 2 only loaded 2a and 2c, while Fig. 8 cuts off the entire right half of the image. I know the figures are complete as I see their full versions in the "Figures" document, just not in the main document.

*The authors **sincerely** thank the reviewer for his continued time and effort in this review process. We have addressed all of the suggestions as noted below. Regarding the Figures issue, we do not see any problems with the round one revision; however, I do see the same issues in the reviewer tracked change docx. Just*

as the last reviewer change docx, I had much issue trying to fix these issues. I believe there may be a possible issue with Word—no matter what changes I make to the reviewer docx, it causes issues elsewhere. Thus, the Reviewer will likely see no changes to the reviewer docx. Nevertheless, I have double and triple checked all figures in the current round two revision and believe they are all good. Additionally, please note that many figures are small now (double column) as some of the changes requested by additional reviewer (3) increased the overall length of the paper.

Major Comment: In the Comparisons and Analysis section, a considerable amount of time is spent discussing the 2003 Stratford, TX tornado from WS04. While I understand the need/benefit to compare to previous work and this is certainly relevant, this section read more like an analysis of data being presented in this paper rather than a simple comparison back to previous work. Several times I had to remind myself that this was data collected by other researchers and not the INPAR. I think this section could be shortened considerably by removing the discussion and description of the observations, and simply highlight the points where the observations compare directly to those collected by the INPAR. This will keep the focus on the INPAR and the data you've worked so hard to collect. As it is there is nearly 2 pages of text before any comparison to the INPAR is made. If the reader needs the detailed description of the data and the tornado, they should be able to go read WS04. In my markup of the manuscript, I've highlighted some general areas in orange that I think are largely unnecessary to the point of this manuscript.

Agreed. I've removed/amended the suggested sections for readability/length.

[Minor comments omitted…]

REVIEWER B (Jana B. Houser):

Initial Review:

Recommendation: Accept with major revisions.

Summary: This study is potentially an interesting contribution to the science, as it has close-proximity pressure, temperature and wind traces during a tornado intercept and a near miss. However, I have several serious concerns that need to be addressed prior to approving this paper for publication. Foremost, the authors are approaching this study with a deliberate intent to find certain features observed in numerical simulations, particularly the vertical vorticity sheet and pressure deficit lobe seen in Leigh Orf's study. While I am a big proponent of Leigh's work and laud his studies for their exceptional visualization, high temporal and high spatial resolution, and their contributions to accelerating our understanding of tornadogenesis, the science contained herein to support the authors' claims is quite weak. Furthermore, hinging an entire paper on simulated features that are found in a single numerically simulated storm representative of one extreme environment (although it was simulated quite extensively) is not ideal, especially considering the limitations of this simulation (particularly that it is frictionless). The evidence presented herein to support the claims of what is being observed in the vicinity of the tornadoes is very circumstantial and the authors' tone is mostly dismissive of other (in my opinion much more likely) alternatives. At times the explanations provided do not provide a thorough explanation of the science.

In its current form, the manuscript cannot be published, but I still think it could be with substantial revision. The motivation and angle need a major overhaul. I would like to see the authors present their observations for face value, and offer a variety of potential hypotheses for what they could be observing. This will require additional work to perform a more thorough literature review to see what else is out there. [As an aside, the lit review is also quite weak. The authors present a sparse representation of the current body of theory and hypotheses and do not demonstrate a thorough familiarity with the current state of the science. The exception is the studies they are choosing to focus on.]

Thank you so much for your helpful and insightful review. While an initial "tough" review is hard pill to swallow, we would like to personally thank Jana, for providing additional scientific insights and thought-provoking ideas, ultimately helping curb our one-dimensional thought processes in early versions of this

manuscript. Thus, her review is much appreciated, and we believe has led to much improvement in our manuscript. We believe we have addressed many of the issues/comments in question. Specific responses to each comment are included below (major points first, followed by specific points).

[Editor's Note: duplicate reply note to first review omitted for space.]

Major Points: Your data are very circumstantial. I think you have a story and you were fishing to find data that fits your story rather than trying to find all possible scenarios and identifying the best one. I would like to see if the science tightened up better. I think the addition of radar observations will hold that. Also, please be open-minded about other possible scenarios that could explain your observations not just the ones you want.

While we do not agree with "fishing for data" verbiage, we understand and respect the reviewer's point. After major revision to most, if not all, sections of this case study, I believe I have tightened up the science substantially.

You are missing a good opportunity to use radar data to supplement your analysis and interpretation of events that happened here.

We understand and appreciate the reviewer's point, please see below.

Why did you outsource to the NWS for your radar analysis? If no one on your team feels comfortable with radar analysis, bring someone in and have them do the analysis and add them as a co-author.

We did not "outsource", it was a detailed collaborative analysis with the KNQA folks to validate our original findings.

The distance to the radar, while a bit far, is still satisfactory for looking for radar-based clues. The beam height is only about 1.5 km ARL, which is on the order of the upper-most reaches of the LLM and you can certainly resolve a new mid-level meso, if one is there.

I have made a major change to this section. The reviewer is correct in that the lowest beam height at 0.5° would be ≈1.5–2 km or ≈4800–5000kft+ at 50–60 nm (which is at best, the upper most reaches of the LLM) at/near 2241 UTC. However, this would be some 5–6 min before the observation of the bowl lowering feature. A lot can happen in 5 min, as the reviewer very well elucidated in Houser et al. (2015, hereafter H15). Additionally, we argue that just because a possible new MLM is or has formed, doesn't necessarily always mean or definitively support the "old" LLM/tornado will/is occluding, cycling or dying (e.g., H15; Wakimoto et al. 1998; Wurman and Kosiba 2013; Davies et al. 1994; Wienhoff et al. 2020; Boustead and Schumacher 2008). While the usual mesocyclogenesis process whether OCM [(e.g., Lemon and Doswell 1979; Burgess et al. 1982; Adlerman 1999; Dowell and Bluestein 2002; Wurman and Kosiba 2012; 2013; French et al. 2013; Droegemeier 2002; 2005) or NOCM (e.g., Droegemeier 2002; 2005; H15) (which are now all cited and referenced)] is usually part of the overall cycling process of the supercell—as the old mesocyclone occludes, the newer mesocyclone further develops. This doesn't mean the "original" LLM/tornado is definitively occluding/dying at that moment (e.g., Boustead and Schumacher 2008; H15).

We have some contention on our end with the exact scientific naming conventions/definitions of the LLM and or MLM with regards to height. For example, where exactly is the lowest portion of the LLM, [especially as it relates to this study (0.5° 4800–6000 kft ARL at 50–60 nm)]? Where does the upper end of the LLM end and the lower portion of the MLM begin? If one could define these exacts, would these arbitrary values be the same for every supercell LLM/MLM? We realize Coffer et al. (2023) give a "rough" comparison defining the LLM near the cloud base as the "low-level" mesocyclone at ≈1 km AGL (and is generally accepted), but they considered this level separate from both the MLM farther aloft "(in the midtroposphere between ≈3 and 6 km AGL) and the "near-ground" rotation that develops much closer to the surface (<250 m AGL; sometimes referred to as the "tornado cyclone"). Even though Coffer et al. (2023) based their study on the LFC as it relates to dynamic upward accelerations, they specify the issues attempting to distinguish exacts between these LLM and MLM levels/values, citing the Markowski et al.

(2008) literature to support. What if the LLM and MLM are vertically or nearly vertically aligned, and what then should we call them? One giant mesocyclone, two independent mesocyclones, two mesocyclones with a tornado cyclone (e.g., Lemon and Umscheid 2008)? While these questions may be rhetorical to some degree, they aren't elementary. Moreover, with the exception of Wood et al. (2017), most LLM/MLM studies have not distinguished between the MLM, LLM pressure-deficit, and the tornado core itself. (Thus, our verbiage of the "mid – LLM" within this study).

Due to the quality of the KGWX radar data due to beam heights ARL, distance, possible attenuation (of the northern mid-LL mesocyclone), we believe the addition of a radar analysis probably doesn't add significant value to this study and appears to "muddy it up" further. [As an aside, I downloaded the Level-2 data, did a brief investigation and indeed, there are 2 mesos at 22:41 at an elevation angle of 1.3°. See below.]

Loads of students are looking for opportunities to contribute to papers and to do this sort of base-level research. Contact me if you need help finding someone… I have several students itching to do research like this!

We sincerely thank the reviewer for the offer! However, the second author of this study is a radar meteorologist, who actually assisted in "cleaning up" some of the noisy RaxPol data from one event back in the day.

While we agree with the reviewer regarding two mesocyclones, we are not confident the "northern" mesocyclone (near 2241) had any meaningful impact to/with the Burnsville bowl lowering as it were (near 2247 UTC on our GPS timestamps) or even the "southern meso" (southwest of Burnsville). Our current thinking, after our second radar analysis, is that the "northern" meso at 1.3° (some 10kft+) only shows burden of proof that the Burnsville supercell likely went through MLM and or LLM cyclogenesis/occlusion (possibly multiple times (we find likely near 2150, 2234, etc.). However, concern exists even at 0.5° (4500-5000kft + at 2241) in attempting to classify the exacts of the LLM or the lower portions of the MLM—where does one begin and the other end? Hence the questions and reference to Wood et al. (2017) posed above. Moreover, we have little confidence observing near-surface low-level features from KGWX near/during the bowl lowering (2247 our GPS timestamps) through the in-situ "deployment" (0.5° near 5000–6200+ kft near 50–60 nm away from KGWX).

I've attached a Level 2 four-panel screen capture (reflectivity, base velocity, Z_{DR}, K_{DP}) at/near 2243 UTC, highlighting distance and height ARL of both mesocyclones. We did find some interesting features through analysis of the Burnsville supercell lifecycle (i.e., multiple dual Z_{DR} arcs at various times – once right before tornadogenesis, weird Z_{DR}–K_{DP} separation angle vectors, a storm-relative velocity enhancement signature (SRVE) feature (when the supercell was closer to KGWX), and while these features are intriguing, we'd be speculating in stating that any of these features were related to the bowl lowering.

In plain language: While we would love to be able to identify, classify and define the exacts of each individual LLM, MLM placement, cyclogenesis etc., throughout the Burnsville event in its entirety, to possibly showcase a misovortex feature like the bowl lowering, we simply can't due to KGWX WSR88D beam height, terrain, etc. Additionally, this is not a radar-analysis case study. We feel somewhat limited in the reviewer's request to define the exacts of the near-surface bowl feature that just might be associated with a LML at near 50–60+ nm away from the radar anywhere from 4900+ to 6000 kft.

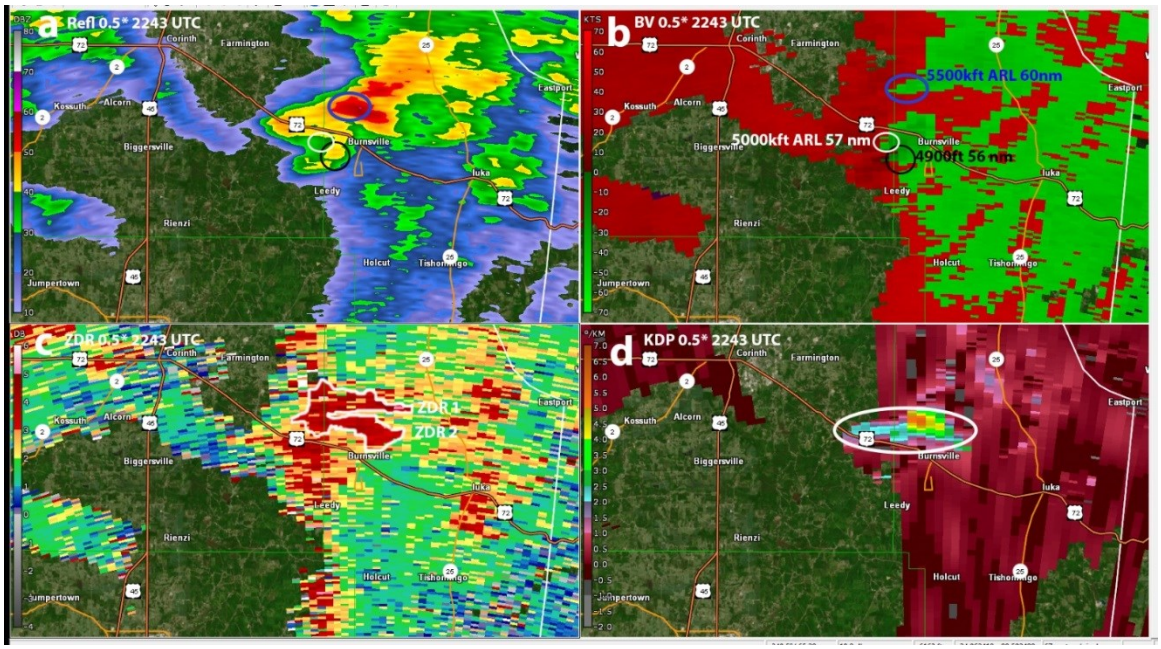

Reply Figure: All at/near 2243 UTC: a) 0.5° base reflectivity. Blue circle showing northern mid-LLM roughly 4 mi north of Burnsville at 5500–6000kft ARL. Small white circle showing possible old BWER. Black circle probable LLM/ongoing tornado at 4900kft ARL at 56 nm. b) 0.5° base velocity showing same as reflectivity with height ARL and distance, c) 0.5° Z_{DR} showing possible two non-disrupted arcs, d) 0.5° K_{DP}.

As alluded to in my overview, I think there are many plausible explanations for what you could be observing and describing throughout this paper that are not necessarily hands down what you are attributing the observations/features to.

Agreed to a point. The reviewer's own formal literature, Houser et al. (2015), highlights dual LLM and tornadoes during the 24 May 2011 El Reno event, that did "not necessarily match a manner entirely consistent with any published conceptual models of cycling", and may be consistent with the non-occluding cyclic mesocyclone (OCM or NOCM; Alderman and Droegemeier 1999, 2002, 2005) and I've expounded and cited this possibility.

I am glad that you eventually mention the possibility of some sort of occlusion process in the Burnsville tornado, although I don't believe this was an occlusion, but rather a new meso forming out ahead of the old one. Typically, occlusions occur further back towards the western portion of the storm, while a new mesocyclone develops out in front of the old one to the north east. As it happens, this is exactly where you are describing it. The positioning that you described matches very nicely with the conceptual model of a cycling super cell (check out Adlerman and Droegemeier's work from the early 2000's.) In such a case, this secondary bowl-shaped lowering would indeed be associated with a mesocyclone, and it would move to the east, as you describe. You can very easily discern that from radar data provided the storm is within close enough proximity to the radar to resolve a smaller scale feature. It is thus entirely possible (probable?) that there could have been a cycling process going on with a second funnel occurring independently of any sort of forward flank convergent boundary or small scale vortices along the boundary. I would personally feel much more comfortable with the claims that you were making if you had additional meteorological context, provided in terms of storm structure (reflectivity) and radial velocity data for the storm at the least.

Please see above.

I don't see the logic behind the argument that dismisses the idea of an occlusion because the first tornado's path is continuous, which you then use as evidence to refute the possibility of the ball shaped feature being associated with another mesocyclone. How does a single damage path possibly rule out the latter? Maybe there was not a tornado with the bowl-shaped feature, but it could very well have still been an intensifying LLM and perhaps even a marginal tornado. I have personally encountered this scenario (i.e. seeing a bowl-shaped lowering, experiencing strong winds beneath it without a formal tornado report) more than once in the field chasing myself.

Agreed. I've removed the entire occlusion discussion as it were.

Another important note about this feature is a scale comparison. The Orf simulations suggest these vortices referred herein as part of the VVS along the forward flank convergent boundary are quite small scale, like tens of meters or so wide. I suspect this feature that you are referring to was likely larger than that which would perhaps argue that it is something else. Based upon the photograph and video data, the scale of this looks much more akin to a low level mesocyclone than a smaller scale misovortex.

While the Orf et al. (2017/2018) simulations do suggest the VVS vortices would be quite small, likely supported in Snyder et al. (2013) and Griffen at al. (2018), we strongly disagree with the reviewer's scale size opinion of the bowl lowering and argue the bowl lowering was/is indeed roughly "tens of meters wide" (i.e., misovortex type), NOT LLM scale. As requested by reviewer #3, I have uncropped the old Fig. 7 (new Fig. 9) and slightly enhanced the contrast to better show the bowl feature size and shape characteristics. We believe the new Fig. 9 (along with the video) clearly show the bowl feature was not an LLM as it appears the reviewer is suggesting. Additionally, we respectfully remind the reviewer that the probe cameras have a 170° field of view (FOV), [which is] very wide. This wide-angle FOV skews the size of objects within the video—especially the closer the object is to the video cameras (this type artifact can be seen in DMH22), and any wide-angle video or still camera lens. In short, the closer the object, the wider it would appear within the video.

Our first observations of the bowl lowering appeared as if [it were] moving easterly, not westerly (in a storm-relative sense), however, due to the reviewer #3 and reviewer #2 comments, and our own questions, I took the video to independent video engineers in Tulsa, OK (one being a meteorologist). We spent 6 h reviewing the entire Burnsville second deployment, particularly the bowl lowering, studying the video frame by frame (29.97–60 fps) from near 2246:54–2247:09 (our GPS time stamps before/during/after the bowl lowering). Results from the three different video engineers (one being a meteorologist) show the Burnsville bowl lowering was rotating cyclonically, and was indeed moving from east to west (i.e., moving westerly toward the tornado), not away from the tornado. Reviewer #3 also makes note of this, and he was not wrong. This can be seen in the video playing it slowly. T his was our mistake that should have been caught. My sincere apologies to all reviewers. Nevertheless, this "finding" also suggests that the Burnsville bowl lowering may not be associated with an LLM cycling phase, and more likely a possible VVS vortex or LRR type (misovrtex), as we continue to believe, and as seen in O17, O18, O20, F18, and Finely et al. (2023). However, because this feature was close to the LLM, as the reviewer correctly suggests, it could be associated with an LLM "occluding mesocyclone" or possibly even a "non-typical non-occluding cycling" phase, as described in Adlerman and Droegemeier (2000, 2005) (cited and referenced), and what is likely seen in the reviewer's own formal literature (Houser et al. 2015) (cited and referenced).

Additional review from the front seat (right side) researcher, indicates "a bowl lowering that was rotating" was observed "looking out the front windshield toward the center left" (i.e., toward the driver's side) of the windshield near 2246:54 (of which her audio can be heard in the video "hurry up,…get it…" near this timeframe). The independent video engineers matched up the researcher's audio to the video and GPS timestamps with an accuracy of ±23 video frames (<1 s with 29.97 fps). This researcher observation and audio timing analysis is critical, because it places a "rotating bowl that was lowering" on the left-hand side (northeast side) of the research vehicle (i.e., just northeasterly if not partially above) at/near 2246:54 ±23 frames. The next visual clue comes roughly 6 s later from the probe video at 2246:59:20 (our GPS timestamp—hours, minutes, seconds, frames), which shows the bowl lowering just to the west of the researchers, moving along Highway 72, as seen in the Burnsville bowl-lowering video. I've attached an

adapted version of the Beck and Weiss (2013) conceptual model below that most resembles our deployment position, with respect to the supercell shape, direction of travel, FFCB/FFDB, LFCB, RFGF/RFDB and tornado core. I've highlighted the rough position of the first observations of a "bowl lowering" from the researcher in the passenger front seat near 2246:54 (via video and audio analysis). I've also highlighted the first probe video observations of the bowl lowering at/near 2246:59:20–2247:05 (our GPS timestamps).

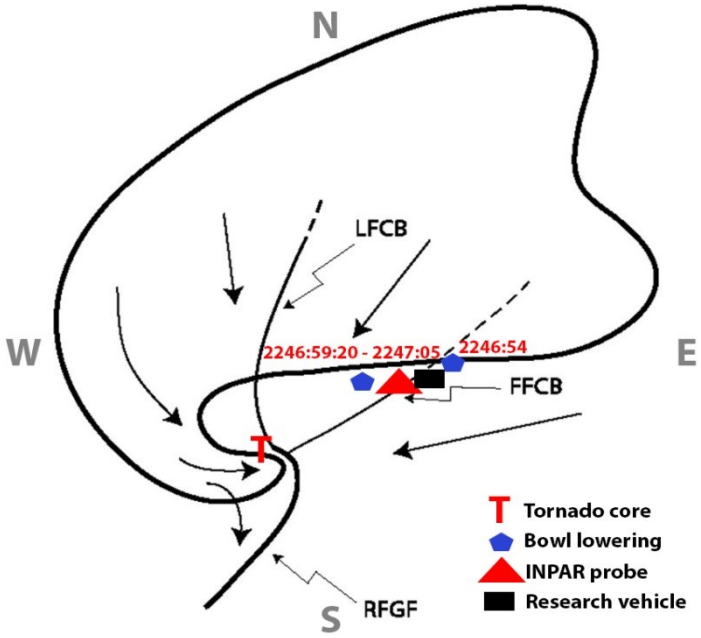

The video engineers were also able to roughly estimate/measure the overall size/width of the bowl lowering starting near 2246:59:20 through 2247:05:20 (hours, minutes, seconds, frames). [Editor's note: Still video captures omitted for space, and in deference to the ethical consideration expressed in the final manuscript.] *The independent video analysis show that at 2246:59:20 the bowl lowering upper width was roughly 12.5 m or roughly 41ft, while bottom portion was roughly 6.9 m. At 2247:00:14, the upper portion of the bowl lowering was roughly 13 m or roughly 43ft, and the bottom portion was roughly 5 m. The bowl lowering at 2247:01:10 [had an] upper width at roughly 14 m or 46ft, and the bottom portion roughly 3 m.*

Of particular importance, in the bottom right of all still images a cell phone tower is noted. While the bowl lowering slightly grew in size, as it somewhat "descended", making it appear as though it was moving toward us, (if it looks like it's not moving but only getting bigger, it is likely moving toward you mentality), the bowl never made it even with, or past the cell phone tower, moving in either a westerly or easterly type direction. Independent video analysis shows that the bowl feature sharply moved toward the right (the north) closer/into the FFD/core just before the view of the feature is lost as the third author (RH), turned the probe slightly toward the Burnsville tornado (southwest of the researchers/Highway 72). At this point, the bowl feature is not seen again. Snyder et al. (2013) LLR observations and particularly the Griffen et al. (2018) observations and follow up study, highlight an inclination ("kink") on/near/close/in the FFDB that would "drag" (for lack of a better word) the LLR vortices further into the core. Assuming these LLR vortices are indeed related to/a part of the VVS, supports the sharp right turn of the bowl lowering deeper into the core (e.g., Griffen 2018). Thus, possibly not related to an LLM cycling phase.

We understand the reviewer is suggesting the Burnsville bowl lowering is associated with or may be the LLM itself. There are four major caveats with this suggestion:

1) Through the entire independent video analysis, the Burnsville bowl lowering never exceeded 14 m or roughly 46ft in width throughout its column. We consider this size comparable to a mesovortex, and not LLM "size" (based on formal lit).
**
2) In 33 years of storm observing, we have never witnessed a LLM that would be this size (this small) and we can find no formal, or even grey literature for that matter, which defines a possible LLM that is this size.

3) The bowl lowering was not/did not move easterly (in a storm-relative sense) with mean storm motion per se. To reiterate, our initial observations were incorrect, likely due to depth perception, conditions during deployment, injury, etc. However, the independent video analysis confirms the bowl lowering was of misovortex size, and that it was along/near the FFCB/FFDB moving westerly, toward the Burnsville tornado. Had it not been for this review process, and getting the independent video analysis complete, we'd likely still hold the same original conclusion, that the bowl lowering was moving toward the east.

4) The formal findings of Snyder et al. (2013) with the Griffen et al. (2018) follow up study, showcases the lifecycles of the LLR. The inclination (kink) occurs on/near the FFDB within the developing stage. The location of the bowl feature correlates very well with the Griffen et al. (2018), Orf et al. (2017; 2018; 2020) and the F23 simulations.

Also, just because the radar was too far away to get good low level data does not supersede the fact that there could indeed be a level mesocyclone there. Please don't dismiss this possibility that just because the radar data are not able to observe such a feature going to the geometry. I am skeptical. (Also, upon investigating the radar data myself, I think I am coming to a different conclusion).

Agreed, and I've offered other possibilities in the revision. Please see above.

It is my opinion that there is a decent amount of superficial text in your narrative that does not ultimately contribute to your storyline and scientific objectives. I challenge you to go back through your paper and identify these parts of the paper and remove them or give them down substantially. Keep your mindset toward the goals of your work and the data you need to supply to prove your hypotheses.

Agreed. I've made major changes to the overall paper including removing superficial text, added additional previous and recent formal literature, amended/changed verbiage throughout, and diligently attempted to tighten up the overall science.

Bottom lines: Reframe your narrative and motivation away from explicitly looking for the features described in Leigh's work. (Even if this was the actual motivation, your results simply cannot substantiate the presence of these features.)

While we respect the reviewer's statement, and agree to a point, we disagree with moving our entire motivation away from the Orf et al. research simply because there is not full consensus throughout the meteorological community. Most respectfully, this request almost seems counterintuitive to the overall promotion and forward progress of the meteorological sciences. Take for example, if not for the early numerical/simulation work of say of Davies-Jones (1984), then Markowski et al. (2012) observations and findings likely wouldn't have come to fruition. Similarly, Houser et al. (2015) observations likely wouldn't have been understood/found if not for explicitly looking at the previous simulation work of Adlerman and Droegemeier (2002, 2005). Nevertheless, I've slightly adjusted our narrative, tightened up the science, discussed other possibilities, and toned down the SVC language.

Add a radar analysis component in addition to your pressure traces so that you can put your locations into broader storm-scale context and analyze the data in terms of velocity and reflectivity structure (you could even include dual-pol data).

Please see above.

Remove superfluous text that doesn't really advance the story or support the scientific goals.

Agreed. I've removed much superficial text for clarity and readability.

Tone down the language about what you are observing. I am not convinced of your story based upon the data presented. There are many possible explanations for what could be happening (you even nicely incorporate many of these explanations yourselves!). Your grounds for dismissal of most of these alternative hypotheses are generally quite weak, and in my opinion, are not sufficiently supported to refute the alternatives in favor of what you are proposing.

I've attempted to "tone down" the overall observational language, added other possible explanations/formal literature, added/amended data presented, removed unfounded science, and attempted to strengthen/explain any dismissal opinions we might have.

[Minor comments omitted…]

Second Review:

Recommendation: Accept with (less-)major revision.

I appreciate the time and effort that the authors took in responding to my review as well as those of the other 2 reviewers. The manuscript is greatly improved as a result of your careful work and your diligence. I sincerely applaud the authors for the efforts exerted. However, there are still several issues that need to be resolved. Many of these are minor and are editorial in nature. As a result, I chose to work directly from the paper itself, using the Word review tools to edit and offer comments/suggestions for improvement. Please do note that some of the comments require a bit of thought and re-working of text. As such, revisions are still required from my perspective. Lastly, thank you (to the authors and the editor!) for your patience with me for the delayed review!

The authors sincerely thank the reviewer for her continued time and effort in this review process and we appreciate the reviewer's suggestions. We have addressed many/most of the suggestion/concerns, as noted below.

[Reply on formatting in minor-comments area omitted...]

Major Comments: I found your consistent introduction of acronyms to be confusing and overused. There are so many it is hard to keep them all straight. As one moves forward into the document, I kept having to look back and find where you defined your acronyms as they are not all commonly used. I recommend only using acronyms for the most frequently used terms.

Agreed. Apologies for any acronym confusion. I've attempted to amended or remove unnecessary acronyms while trying to keep only the most important. My apologies if I've missed any. We understand the Reviewer had concerns with the use of the VVS, PDL etc. in the round-one review. As stated in the author replies from round one, the VVS was/is used extensively in Orf et al. 2017; 2018; 2020, and Finley et al. 2018; 2023, as well as other lit. The UDI was used in our last formal (e.g., DMH22) and used extensively by the NWS. The LLM, FFCB, FFDB, RFDB has been used in a plethora of formal lit for years (likely too many to cite here). Thus, please do note, we continue to use the PDL, VVS, FFDB, FFCB, RFDB, etc. throughout. However, I've tried to clean up redundant acronyms or places where I should have used them instead of actually writing them out followed by the acronym (and vice versa). We hope this is to the Reviewers satisfaction. Another thought that just occurred to me: it might be possible to add an additional Appendix listing the associated acronyms if this may help? Of course, this is likely dependent on the Editor and length of the paper. It is our understanding that EJSSM manuscript length limits are 32 pages, and with the current changes the reviewer is suggesting, may put us close or over that limit.

There are still some issues with the introduction that need to be remedied. I found the material to be disorganized, particularly the last page or so of the intro and then sporadically through the presentation of your cases/results.

Agreed. I have diligently attempted to clear up further areas of disorganization in the Introduction and throughout. Direct comment to the Reviewer: We very much appreciate your suggestions/edits offered in the docx sheet in this section. They were very helpful, especially to newer authors such as ourselves. Please note though, the reviewer's request to modify or move the subsection (a) in the Introduction has not changed. During the first-round review, reviewer #1 recommended adding that subsection to lightly introduce past in-situ observations, which we agreed. We feel the manuscript flow is sufficient through this part of the section. Although, please note, we have added the reviewer's recommended suggestion regarding "owning to the pressure field in the forward flank", and then changed the subsection (a) to: "Background—past pressure observations". We believe this change, as well as others throughout, have substantially helped with organization, clarity, readability, and overall flow.

I also think there is still room for improvement in your description of your instrumentation. I understand that you are referencing another one of your works, but you are also going into some detail here as well.

Agreed to a point. [Importantly] we are not just referencing one of our previous works, but also the Samaras and Lee (2004) lit. We believe that understanding the Samaras and Lee (2004) literature in a reviewer capacity is critical to understanding the wind-tunnel test results, the X/L, C_p, and the recorded data/results from the three events described. I've attempted to lightly change some verbiage regarding instrumentation to hopefully help the reviewer understand. Because reviewer #1 and reviewer #3 found no additional issues with the instrumentation descriptions from the last revision, with reviewer #3 "Accept" recommendations, and reviewer #1 "accept" with only one minor issue (not related to the instrumentation or explanation of such), I'd hate to make major or even multiple minor adjustments here - taking two steps back for one step forward if you will. But for the sake of this reviewer, in addition to adding the point [Fig. 2a (old Fig. 1a)] in the round-one revision, I've lightly adjusted explanations in this section. I've also used references in addition to assertion with explanations.

Regarding the X/L, C_p, and associated "values", and wind tunnel data/results, this is not new theory with regards to in-situ probes. Samaras and Lee (2004), which is cited and explained (in detail) along with our own previous formal lit (Dean et al. 2022), which provide clear definitions and we believe answers/addresses most, if not all, of the reviewer's questions/concerns. Therefore, we very, very respectfully ask the reviewer to familiarize herself with the Samaras and Lee (2004) lit.

I still think your writing at times is a little too speculative in an effort to boost what you are hoping to prove. I commented in the tracked changes document where I thought this particularly needed to be addressed.

Agreed to a point. I've made much of the reviewer's recommended changes listed to cut down on the speculation.

There are also places with the content is still a bit disorganized. For example, you talk about one thing, then talk about another thing, then return to thing #1. Please be mindful to consolidate topics so that you are only talking about them once or sequentially in a temporal sense. Comments in the document highlight these areas, but I encourage you to go back through with this in mind and reorganize as appropriate.

Agreed to a point, and I've made multiple light changes throughout, including rearrangement of one section, as the reviewer suggests, and removing/amended much of another section suggested by reviewer #1 (this would be part of the WS04 pressure-trace section).

[Minor comments omitted…]

REVIEWER C (Kelton T. Halbert):

Initial Review:

Recommendation: Accept with major revisions.

General Comment: I'd like to start with the positives first. The authors have done a very thorough job describing their instrumentation, design, calibration, testing, validation, and comparisons with other similar observation platforms. While instrumentation design and implementation is not my specialty, I feel like the authors have done more than their due diligence in ensuring that the measurements are quality enough to compare with other sensor probes used in this manner. To me, this is the bigger and harder hurdle to clear, so well done on doing everything from wind tunnel tests to mesonet comparisons. The comparisons to other pressure logging probes placed in the vicinity of tornadoes was thorough, and I couldn't find any fault with the comparison and analysis between these different observations and platforms.

I do have some comments, concerns and suggestions that I would like to see the authors address. Most of the nitty-gritty details are in the .docx comments, so below are a few overarching things I noticed.

Thank you so much for your helpful and insightful review, which we believe has led to much improvement from earlier versions of our manuscript. Due to Kelton's history, study, research, and deep understanding of the SVC and related features via simulation work with Dr. Orf, his review/comments are most especially important to this case study and are very much appreciated. We believe we have addressed all or most issues/comments. Specific responses to each comment are included below (overarching replies first, followed with the docx. replies). [Editor's note: duplicate note to other replies is excluded here for space.]

Substantive Comments, Overarching: Section 3 (Tornado case descriptions): Other reviewers and the editor may have different opinions, so this isn't a hard stop on the paper, but I personally feel that large sections of Section 3 can be trimmed down to improve the readability and focus of the paper. Right now, they read like full day chase logs, and while thorough, not all of those events and descriptions pertain to the recording and analysis of data. The photogrammetry attempt isn't really used anywhere else and isn't super thorough, for example.

We believe reviewer #3 actually means Section 4 (Case events), not section 3 (Probe operating principle)? Agree. I've amended much of Section 4 (Case events) including a few figures: removed old Fig.5b due to redundancy, removed old Fig. 8b (inflow schematic), and removed the entire photogrammetry section. I've also rewritten or modified much of this section to help readability, flow and focus of the paper.

Along these lines, while I admire the forthrightness about the close encounter with the Burnsville tornado and using it as a teaching moment, its inclusion in the paper feels unnecessary to me. However, I will leave it to the Editor and other reviewers to determine whether or not these changes would be necessary for publication.

We strongly but respectfully disagree with removing the Burnsville event/close encounter. We believe that many of the Burnsville observations are not only a good teaching opportunity, but also may include important features/observations (including those that may seem trivial) that are likely relevant to the "possible" SVC (e.g., LFCB, FFCB, inflow etc.) and our possible position to these particular features. While the means of obtaining the Burnsville data wasn't "pretty", we believe it is still very valuable data for any future studies/publications. However, I have removed mention of being struck by the Burnsville tornado in the Introduction (as recommended by reviewer #1) and have carefully and methodically attempted to weave this into/around the remainder of the paper. We agree that our efforts to be as thorough as possible (also noted by reviewer #2) have forced the Burnsville case in this study to read somewhat like a chase day log. However, review of the Blair et al. (2008) literature (published in this journal) and the Lee et al. 2004 literature, also could be read as such. Nonetheless, I've removed much of the "chasing blog" type format and tightened the science substantially throughout. We believe there is much scientific merit in the remaining first-person scientific and video observations, which seem especially important considering the lack of these types of in-situ observational data since 2013.

Section 6 placement: It is my personal opinion that section 6 could be combined with section 2, since the data validation in the wind tunnel and with the mesonet feel related enough to be combined. It may require some extra work reformatting it to flow well with describing the impacts of the partial car deployment, but I believe it would improve the logical flow of the paper.

Agreed. I've combined old section 6 with section 2 and have rewritten/amended much of section 2. This rewrite forced us to move old Fig. 14 to new Fig.4 and old Fig. 15 to new Fig. 5a (and associated 5b). Two new equations were also added for full-scale (FS) testing elaboration (with remaining figures/equations following suit). Additionally, I've written/added a new section 6 (Theoretical concerns and observational considerations) discussing the impacts of the Burnsville "partial" deployment and possible issues with Cp, XL and angular dependence.

Improvements to figures and equations needed: Figure 3, Fig. 5, and Eqs. 1 and 2 are a little bit under-baked. The figures in particular could use some reformatting to make more efficient use of space in the paper, and the equations are on the low-resolution side and mixed between LaTex and normal keyboard format. It would be appreciated to generate higher-quality equation images and to format all of them in LaTex-style for readability purposes. Finally, while mentioned in the review document, Fig. 7 could use some updating or modification to make the bowl feature more visible to the reader.

Agreed. I have attempted to "re-bake" the old Figs. 3, 5 and 7. Old Fig. 7 (new Fig. 9) has been replaced with the original (uncropped) video screen capture, and I've increased contrast, tone, and size slightly. As mentioned above, I've also added equations as requested and rewritten all equations to hopefully help quality and format.

Substantive Comments, Scientific: Identification of storm-scale features: For the most part, the authors do a reasonable job about leaving certain things as inconclusive in their identification due to lack of data. However, there are a few sections where the scientific justification and logic don't quite support the claims being made. Not in that they are patently false, but because they don't quite exceed the burden of proof required for definitive claims. I don't think that it prevents the paper from publication, but does require some editing to make these uncertainties in interpretation a little more clear. With the absence of radar data analysis (or quality radar data, as is the case in the Burnsville event) in the paper, and the fallibility of human assessment of storm-scale features, it's just a good precaution to be a little more open-ended with some of this. It is especially challenging since it is near impossible to determine smaller-scale storm features using a pressure trace alone, since many things can serve to lower/raise pressure within a supercell (strengthening/weakening mesocyclone, vortices, boundaries, etc).

Agreed. I've attempted to clear up the justification and scientific logic in rewriting or amending most all sections. I've removed the tornado/inflow boundary layer and the Kosiba and Wurman reference/citing. I've attempted to either clarify or be much more open-ended/tone down the language with regards to storm-scale features, particularly the SVC (as strongly recommended by reviewer #2.). I've amended verbiage to include "possible SVC", or "possible SVC location" etc. throughout.

Additional citations: There are a few sections scattered throughout the paper that could possibly use some further citation or elaboration. Some of these claims may be considered common knowledge, but I would appreciate revisiting some of them and making sure that those claims can be properly and thoroughly backed up. This also includes the need for citation for any software libraries used in the development of the probe or in the analysis of the data, or even in the citation of the wind tunnel used (if available).

Agreed. I've added numerous citations throughout (e.g., Oklahoma mesonet; Brock et al. 1995; National Research Council 2009; McPherson et al. 2007 and multiple others), and external links, (e.g., full-scale pressure-sensor calculations, software libraries etc.) or elaboration throughout.

Descriptions of the streamwise vorticity current: There are several sections that make reference to the SVC as if it is a known fact that it is present within the storm being analyzed, but as of now, it is unknown what percentage of tornado producing supercells have an SVC, or if an SVC is even required to be present at all. Because of this, it would be more appropriate within the analysis to use phrasing such as "the possible/probable location of an SVC, if present". Unfortunately, without RHI radar cross sections, it is

really hard to identify the presence of an SVC, even if cloud features are present that indicate one may exist. I'm pretty sure the TORUS field catalog has some radar data from the McCook, NE tornado day that may help prove the presence of an SVC, or perhaps there are publications post-TORUS that can be cited that say so. This may feel nitpicky, but it's an appropriate caveat that needs to be said when undertaking scientific analysis of the data.

Totally agreed. I've amended verbiage to indicate the unknown percentage of supercells having an SVC etc., and made changes to reflect the "possible SVC" verbiage accordingly (I am trying to tone down the SVC language as requested by reviewer #2). Additionally, I cited the 2019 TORUS field catalog for the McCook event. We will likely never know for certain if the Burnsville supercell had an SVC, despite our continued belief is that the Burnsville bowl lowering is likely an SVC VVS vortex.

While an SVC was documented in great detail during McCook event Satrio (2023), he also traced parcel trajectories "backward" and not only found concrete evidence of the SVC, but also vorticity budgets showing strengthening of the McCook, NE, LLM with parcels that originated within the forward-flank region of the McCook supercell (i.e., along and behind the FFCB/FFDB), proving that the SVC is legitimately physical. Still, it is unknown what percentages of supercells actually have an SVC or what role, if any, the possible SVC might have on the LLM, tornadogenesis, maintenance, or decay, and we have stated this verbatim.

While I assume reviewer #3 is aware, I doubt the rest of the reviewers/editor are. Through heavy personal discussions and collaboration with Dr. Orf, following our dataset of the Burnsville event, he successfully placed ground-based "location pressure probes" within his El Reno simulation, near/in the same areas of our "real world" observations (e.g., VVS; PDL "the death banana"). I believe his findings were eerily similar to our "real world" findings, which I think might possibly be showcased in the future-–I do not know that for certain--hence, the reason I initially did not use more open-ended verbiage. This was also likely due to author sloppiness on my part. As mentioned above, I believe I have now corrected the reviewer concerns.

Uncited/undescribed error metrics (section 6): In section 6, the percentages are mentioned without context as to what they are. Presumably, they are error percentages, but there's no equation or process description of the percentage. Because of this lack of clarity, I believe the error metrics to be slightly erroneous, as the numbers don't quite match the best-practice error metric used for pressure sensors using the full scale (FS). It doesn't severely impact the scientific interpretation of the data, but at best it's vague and needs clarification, and at worst, using the wrong metric to calculate sensor error. Additionally, the probe data are compared to the mesonet, but I did not see any citation of the Oklahoma Mesonet or description of the sensors being compared to, making it hard to fully contextualize the comparison. The Oklahoma Mesonet has a paper citation that should be a part of this analysis.

Agreed. The original calculations were indeed "truth test" errors that allowed us to get our foot in the door at the wind tunnel. However, I've amended/included the correct FS metric error with equations (formatted) and citation/reference. As mentioned above, I've added citations, references, or in-text links such as the Oklahoma Mesonet, etc. where appropriate.

[Minor comments omitted…]

Second Review:

Recommendation: Accept.

General Comment: Thank you to both the author and the editor for your patience in the reviewing of this manuscript. Having read the review replies and the revised edition of the manuscript, I am very pleased with the current state of the logic, flow, citations, and claims made wtihin the paper. The scope feels more well defined, and the authors have adequately addressed all concerns and changes indentified in the review process. With this in mind, I see no problems in accepting this article for publication.

The authors very much appreciate Kelton's time and patience through this review process. Please note: a few things have changed, such as figures are small now (double column) and multiple minor changes requested by [another] reviewer. Again, we thank the reviewer for his time.